

Article

Control Mechanism and Support Technology of Deep Roadway Intersection with Large Cross-Section: Case Study

Zaisheng Jiang¹, Shengrong Xie^{1,2}  and Dongdong Chen^{1,*}

¹ School of Energy and Mining Engineering, China University of Mining and Technology-Beijing, Beijing 100083, China; zaisheng_j@163.com (Z.J.); xsrxqc@cumtb.edu.cn (S.X.)

² Beijing Key Laboratory for Precise Mining of Intergrown Energy and Resources, China University of Mining and Technology-Beijing, Beijing 100083, China

* Correspondence: chendongbcg@cumtb.edu.cn

Abstract: Conventional bolt–shotcrete support technology is usually single-layered, which does not meet the requirements of strength and stiffness for roadway support. Therefore, in this paper, new combined support technology, including a multiple-layered staggered dense arrangement of bolts, multiple-layered laying of steel meshes, multiple-layered pouring of shotcrete, strengthening support of long cables, and full cross-section grouting, is proposed. Specifically, the following new combined support technology process is proposed: first layer of shotcrete (80 mm), first layer of mesh, first layer of bolt, second layer of shotcrete (50 mm), second layer of mesh, second layer of bolt, reinforced cable, third layer of shotcrete (50 mm), and grouting. The results show the following: (1) In the system of a superimposed coupling strengthening bearing arch, compared to a cable bearing arch, changing the support parameters of the bolt bearing arch can significantly vary the bearing capacity. A range of bolt spacing between 0.4 m and 0.7 m is more conducive for a high performance of the bearing capacity of the superimposed coupling strengthening bearing arch. (2) With the increase in the single-layer shotcrete thickness (from 50 mm to 100 mm), the bearing capacity of the shotcrete structure increased rapidly in the form of a power function. (3) After the multi-level bolt–shotcrete support structure was adopted, the ring peak zone of the deviatoric stress of the surrounding rock at the roadway intersection was largely transferred to the shallow part, and the plastic zone of the surrounding rock of the roadway was reduced by 43.3~52.3% compared to that of the conventional bolt–shotcrete support. The field practice model showed that the final roof-to-floor and rib-to-rib convergences of the roadway intersection were 114 mm and 91 mm after 26 days, respectively. The rock mass above the depth of 3 m of the roadway’s roof and sides was complete, the lithology was dense, and there was no obvious crack. The new technology achieves effective control of a deep roadway intersection with a large cross-section.

Keywords: deep mine; roadway intersection; multiple bolt–shotcrete support; bearing arch; combined support



Citation: Jiang, Z.; Xie, S.; Chen, D. Control Mechanism and Support Technology of Deep Roadway Intersection with Large Cross-Section: Case Study. *Processes* **2023**, *11*, 1307. <https://doi.org/10.3390/pr11051307>

Academic Editors: Junwen Zhang, Xuejie Deng and Zhaohui Wang

Received: 20 March 2023

Revised: 5 April 2023

Accepted: 21 April 2023

Published: 23 April 2023



Copyright: © 2023 by the authors. Licensee MDPI, Basel, Switzerland. This article is an open access article distributed under the terms and conditions of the Creative Commons Attribution (CC BY) license (<https://creativecommons.org/licenses/by/4.0/>).

1. Introduction

China’s “lack of gas, less oil and relatively rich in coal” resource occurrence characteristics have determined that coal will still be the leading source of energy in China for a long time in the future [1,2]. In order to ensure the energy supply, researchers have conducted a lot of research on the prediction and control of various disasters in the field of coal mining [3–5]. In addition, in China, the coal mining depth is increasing continuously with the exhaustion of shallow coal resources [6–8]. With the increase in the mining depth, the stress environment of the surrounding rock becomes more complex, and it presents the characteristics of a soft rock, which makes surrounding rock control of a deep roadway more difficult [9–11]. As the throat part of mine transportation, the cross-section of a roadway intersection is large [12,13]. Simultaneously, it is affected by stress concentrations and

engineering disturbances, resulting in poor support conditions and frequent renovations of the roadway intersection [14–16]. Owing to the high transport capacity of a modern mine, there are numerous roadway intersections in a deep mine. Therefore, studying the stability of the surrounding rock at a deep roadway intersection with a large cross-section has become an urgent technical problem in modern mines.

As an essential part of deep roadway support technology, bolt–shotcrete support technology plays an important role in controlling the surrounding rock of a deep roadway [17,18]. In fact, in deep complex environments, when roadways are subjected to the superimposed effects of static and dynamic loads, one of the most common methods to ensure the stability of the surrounding rock of a deep roadway is to use bolt and anchor cable for reinforcement [19,20]. Shotcrete can quickly seal the surrounding rock, which is often prepared with admixtures, such as cement, sand, stone, and mineral admixtures, such as fly ash, ultra-fine slag, and silica fume [21,22]. On the basis of the above, a super early strength agent composed of fast-setting early-strength components and water-reducing components can be added to prepare fast-setting and rapid-hardening high-strength shotcrete [23]. In recent years, scholars have realized numerous beneficial achievements in deep roadway bolt–shotcrete support technology. Malmgren et al. investigated the influence of the following factors on bolt–shotcrete support: shotcrete thickness, bolt parameters, rock strength, and Young’s modulus, and the mechanical properties of the interface of the shotcrete, rock, and bolts [24]. Sjolander et al. proposed a numerical model for simulating the failure of bolt anchorage and shotcrete, which includes the pull-out failure of bolts, cracking of the shotcrete, and bond failure between the shotcrete and rock [25]. Naithani et al. implemented 3D engineering geological mapping for a project roadway and proposed combined support technology including bolt, steel fiber-reinforced shotcrete, drainage hole provisions, and grouting [26]. Basarir et al. analyzed the stability of the gateway of a deep mine and proposed a support system composed of a bolt, a cable, and shotcrete [27]. Panda et al. analyzed the rock mass properties for an optimum support system and proposed a combined reinforcement method for surrounding rock, including 3.0–4.4 m of bolts, 0.1–0.15 m of shotcrete, wire mesh, and a final concrete lining [28]. Yu et al. suggested a mechanical model of an overlap arch-bearing body, which was composed of a main compression arch (bolt support) and a second compression arch (cable support) [29]. The above scholars augmented the research results of deep mine bolt–shotcrete supports. However, bolt–shotcrete support technology has usually been a single-layered arrangement in previous studies. In addition, researchers have scarcely studied multiple-layered bolt–shotcrete superimposed coupling strengthening bearing arch support technology and its surrounding rock control mechanism. The difference between this technology and conventional single-layered bolt–shotcrete support technology lies in the multiple-layered staggered dense arrangement of bolts, multiple-layered laying of steel meshes, and multiple-layered pouring of shotcrete. The difference between this technology and conventional single-layered bolt–shotcrete support technology is shown in Figure 1.

Taking a roadway intersection with a large cross-section buried more than 800 m deep in the Xingdong coal mine as the engineering background, we comprehensively utilized several research methods, such as on-site geological investigation, numerical simulation, theoretical analysis, engineering practice, and on-site rock pressure measurement. The failure characteristics and mechanisms of the roadway intersection were investigated, and new combined support technology, including a multiple-layered staggered dense arrangement of bolts, a multiple-layered laying of steel meshes, multiple-layered pouring of shotcrete, the strengthening support of long cables, and full cross-section grouting is proposed. In addition, the supporting mechanism of the new technology is revealed, the numerical calculation models for roadway intersections under different supporting conditions are established, and the engineering applicability of the new technology is verified. The field engineering application results show that this technology can significantly limit the deformation of the roadway’s surrounding rock.

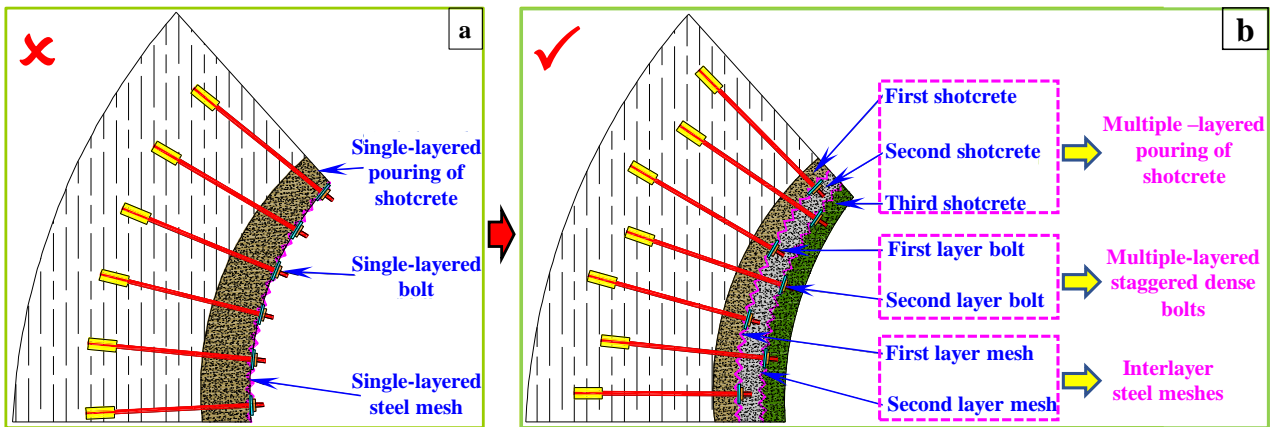


Figure 1. Comparative differences between conventional and multiple-layered bolt-shotcrete structure. (a) Conventional single-layered bolt-shotcrete structure, (b) high-strength anti-crack and anti-bending bolt-shotcrete structure.

2. Project Background

2.1. Project Overview

The Xingdong coal mine in Xingtai City, Hebei Province, China, has two working levels. In this study, a -760-m -level roadway intersection was selected, as presented in Figure 2a.

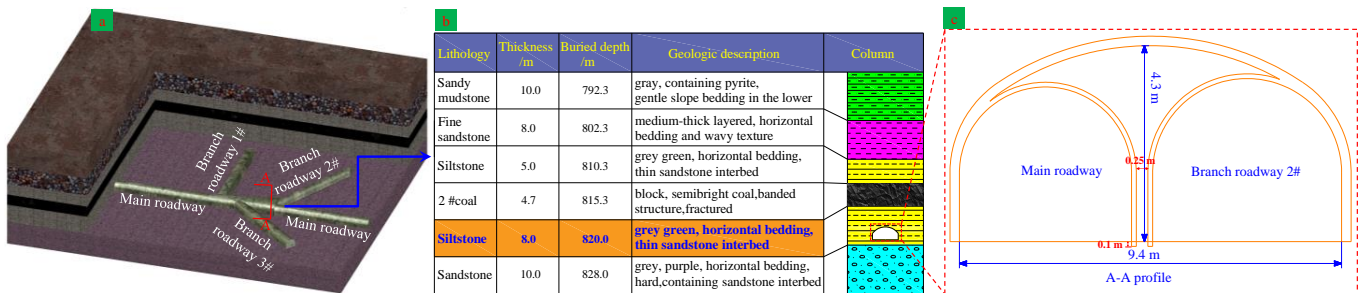


Figure 2. (a) Roadway layout, (b) strata histogram, (c) the intersection with the largest section.

The roadway intersection is arranged on the floor of the No. 2 coal seam, which is buried deeper than 800 m. A detailed strata histogram is illustrated in Figure 2b. The maximum cross-section of the roadway intersection has the shape of a straight wall and an arc arch with a width of 9.4 m and a height of 4.3 m (see Figure 2c).

2.2. Primary Support Scheme and Strata Behavior Characteristics

The primary support of the roadway intersection is a conventional single-layered bolt-shotcrete support. The support parameters are as follows: bolt: $\varphi 22 \times 2000$ mm, spacing: 800×800 mm; cable: $\varphi 21.8 \times 6500$ mm, spacing: 2000×1800 mm; grouting bolt: $\varphi 22 \times 2000$ mm, spacing: 1500×1500 mm; shotcrete: 120 mm. After the implementation of the primary support scheme and parameters, the roof-to-floor and rib-to-rib of the roadway underwent continuous large convergence (see Figure 3a). Numerous support materials were broken after their initial installation, as shown in Figure 3b, which severely affected the mine’s transportation and regular production. Therefore, it is urgent to develop a new support scheme for this roadway intersection.

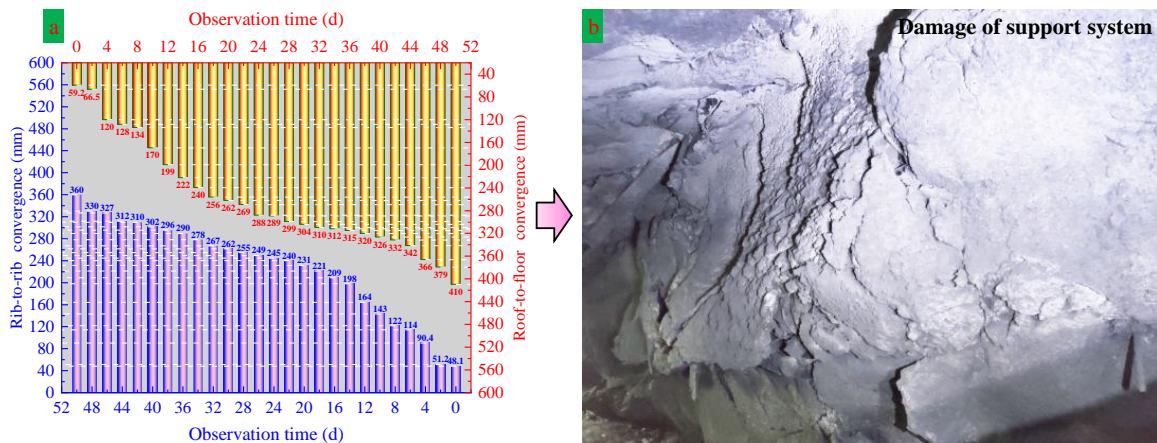


Figure 3. (a) Convergence of surrounding rock under the primary support method, (b) deformation and failure of surrounding rock.

2.3. Failure Mechanism Analysis of Roadway Intersection

Briefly speaking, a roadway intersection at a large buried depth has a large cross-section span. In addition, the surrounding rock mass is significantly affected by the engineering excavation. In the case of unreasonable primary support, deformation of the whole cross-section and failure of the surrounding rock at the roadway intersection are more prominent. The causes for the failure of a roadway intersection are shown in Figure 4.

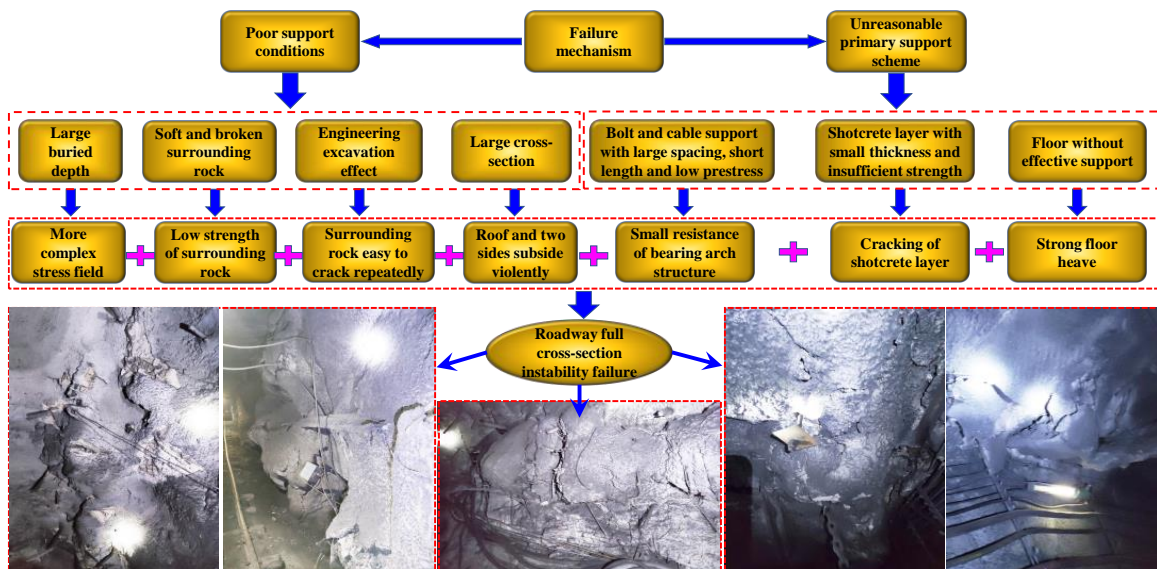


Figure 4. Failure mechanisms of roadway intersection.

3. New Combined Support Technology

Therefore, in view of the damage of the roadway intersection buried deeper than 800 m at the Xingdong coal mine under a conventional single-layered bolt–shotcrete support, the following new combined support technology process is proposed: first layer of shotcrete (80 mm), first layer of mesh, first layer of bolt, second layer of shotcrete (50 mm), second layer of mesh, second layer of bolt, reinforced cable, third layer of shotcrete (50 mm), and grouting. This new support technology comprises a multiple-layered staggered dense arrangement of bolts, multiple-layered laying of steel meshes, multiple-layered pouring of shotcrete, strengthening support of long cables, and grouting reinforcement of the surrounding rock.

3.1. Superimposed Coupling Strengthening Bearing Arch Support Technology and Mechanism

The technology of superimposed coupling strengthening bearing arch formation using multiple bolt–shotcrete layers is shown in Figure 5.

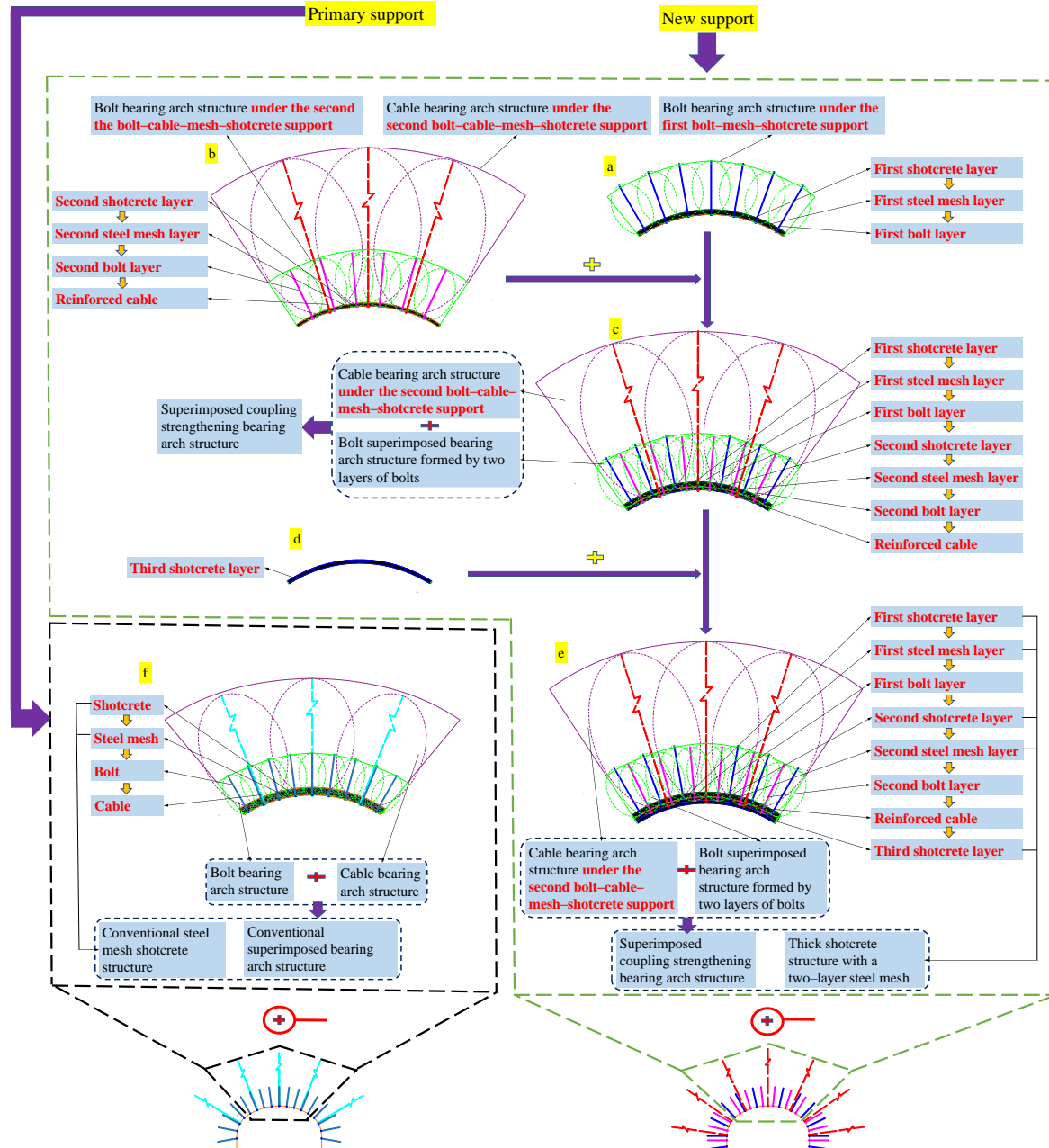


Figure 5. Multiple bolt–shotcrete support technology and primary support. (a) First bolt–mesh–shotcrete support, (b) second bolt–cable–mesh–shotcrete support, (c) superimposed coupling strengthening bearing arch structure, (d) third shotcrete, (e) final new support effect formed, (f) primary support effect.

Specifically, first, workers apply shotcrete to plug the surrounding rock after the excavation of the roadway intersection, lay the first steel mesh, and install the first layer of bolts (this stage is the first bolt–mesh–shotcrete support, as shown in Figure 5a). Subsequently, the workers apply the second layer of shotcrete, lay a second layer of a steel mesh, install a second layer of bolts, and install a reinforced cable (this stage is the second bolt–cable–mesh–shotcrete support, as shown in Figure 5b). The support effect formed

by two bolt–shotcrete layers is shown in Figure 5c. Finally, the third layer of shotcrete is implemented, as shown in Figure 5d. The support effect after the third layer of shotcrete is shown in Figure 5e. Compared to the primary support (see Figure 5f), in the new support (see Figure 5e), the thickness of the superimposed coupling strengthening bearing arch is larger, the influence range is wider, and the bearing capacity is higher. In addition, in this new combined support technology, pouring shotcrete thrice and laying the steel mesh twice can form a thick shotcrete structure with a two-layer steel mesh, which improves the shotcrete structure’s mechanical properties significantly and plays a role in maintaining a two-layer bearing arch. In this study, to distinguish between the action mechanisms of a bolt and a cable, the bearing arch formed by bolts is called a bolt bearing arch, and that formed by cables is called a cable bearing arch. The bearing arch formed by two layers of bolts is called a bolt-superimposed bearing arch.

When the first bolt–mesh–shotcrete support is implemented, the compressive stress zones between adjacent bolts are superimposed, forming a bearing arch structure. In the initial stage of roadway excavation, the bearing arch structure using a shotcrete layer could seal and support the broken surrounding rock in time. A sufficient prestress offered by the bearing arch structure improves the roadway’s confining pressure. FLAC3D software simulated the three-dimensional spatial stress and the profile stress distribution of the bearing arch under the first bolt–mesh–shotcrete support, as shown in Figure 6a–c.

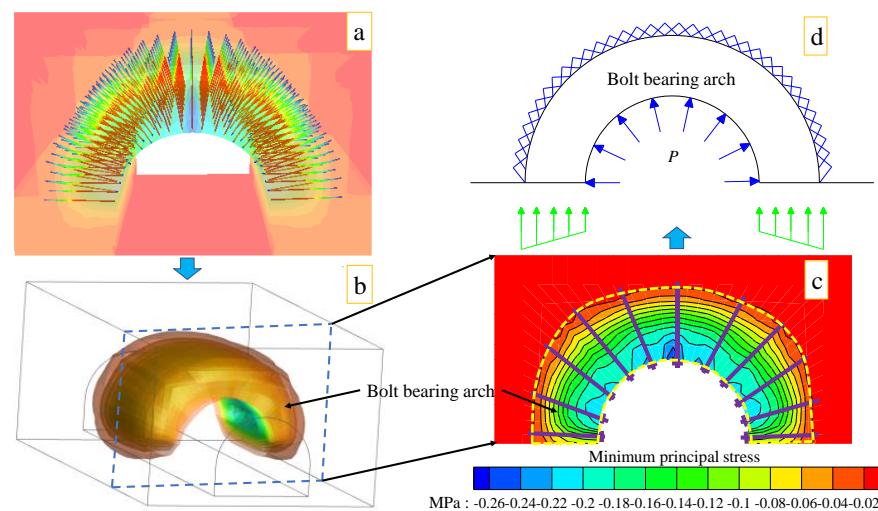


Figure 6. Bearing arch structure under first bolt–mesh–shotcrete support. (a) Spatial arrangement of bolt, (b) three-dimensional spatial stress distribution of bearing arch, (c) profile stress distribution of bearing arch, (d) mechanical model of bearing arch.

After a certain degree of deformation, pressure is released from the surrounding rock, and the second bolt–cable–mesh–shotcrete support is implemented. The bearing arch structure formed by the bolts and reinforced cables in the second bolt–cable–mesh–shotcrete support (the three-dimensional spatial stress and profile stress distribution of this bearing arch are shown in Figure 7a–c) is superimposed, with the bearing arch formed by the bolts in the first bolt–mesh–shotcrete support. This will form a superimposed coupling strengthening bearing arch structure with high strength, strong bending, crack resistance, and reasonable stress distribution, which prevents further deformation of the surrounding rock.

Owing to the complexity of the superimposed coupling strengthening bearing arch structure in practical engineering, to facilitate the stress analysis of its bearing capacity, the following assumptions were made: (1) The surrounding rock at the roadway is approximately isotropic, homogeneous, and continuous. (2) After a two-layer bolt–shotcrete, the surrounding rock mass is still regarded as an elastic–plastic medium. The failure of the rock mass follows the Mohr–Coulomb criterion. (3) The arch section of the roadway

is approximately semicircular. (4) The restraint resistance of each bolt (cable) is evenly distributed in the surrounding rock circle.

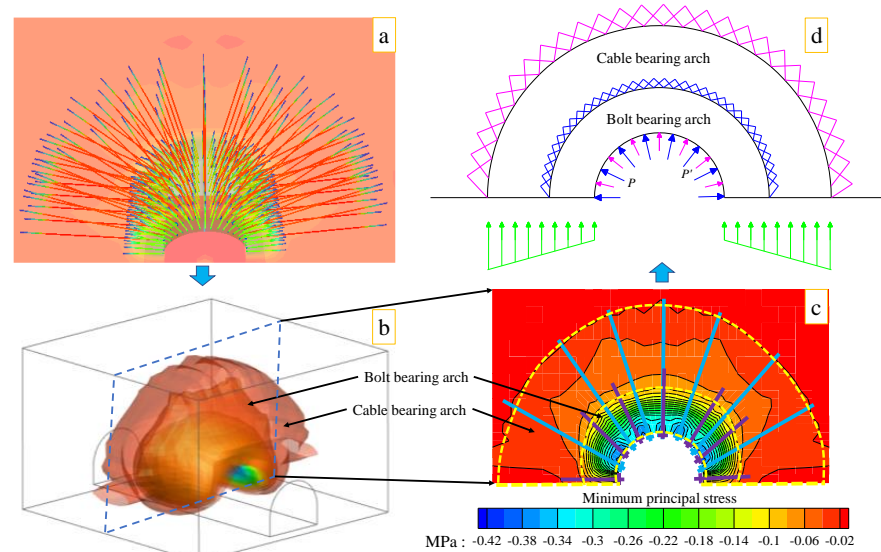


Figure 7. Bearing arch structure under the second bolt–cable–mesh–shotcrete support. (a) Spatial arrangement of bolt and cable, (b) three-dimensional spatial stress distribution of bearing arch, (c) profile stress distribution of bearing arch structure, (d) mechanical model of bearing arch.

Combined with the above assumptions, specific mechanical models were established. The bearing arch mechanical models under the first bolt–mesh–shotcrete support and the second bolt–cable–mesh–shotcrete support are shown in Figures 6d and 7d, respectively. P is the restraint resistance provided by the bolt, and P' is the restraint resistance provided by the cable.

Following the first bolt–mesh–shotcrete support, the roadway's surrounding rock still follows the Mohr–Coulomb strength criterion under the limit equilibrium as follows:

$$\sigma_1 = \sigma_3 \frac{1 + \sin \varphi}{1 - \sin \varphi} + 2c \frac{\cos \varphi}{1 - \sin \varphi} \quad (\text{MPa}) \quad (1)$$

where σ_1 and σ_3 are the maximum and minimum principal stresses in the rock mass (MPa), respectively, φ is the rock internal friction angle of the loosely broken zone in the surrounding rock ($^\circ$), and c is rock cohesion of the loose zone in the surrounding rock (MPa). When the surrounding rock does not have a support, the rock in the loose zone is in a broken state. From the perspective of conservation and safety, c is 0. Therefore, Equation (1) becomes

$$\sigma_1 = \sigma_3 \frac{1 + \sin \varphi}{1 - \sin \varphi} \quad (\text{MPa}) \quad (2)$$

when the stress state of any point of the surrounding rock in the bearing arch satisfies Equation (2), the surrounding rock will enter the failure state. The stress in the inner surface of the roadway's surrounding rock is generally equal to the restraint resistance: $\sigma_3 = P$.

The P relationship with the bolt support resistance is as follows:

$$P = \frac{F_b}{D^2} \quad (\text{MPa}) \quad (3)$$

where F_b is the bolt support resistance (kN), and D is the bolt spacing under the first bolt–mesh–shotcrete support (m).

To calculate the bearing resultant force, N , of the bearing arch on the unit length along the axial direction of the roadway, the following differential relationship is used:

$$ds = \left(r + \frac{b}{2}\right)d\theta \quad (4)$$

where ds is the arc differential length unit of the bearing arch center, r is the roadway radius (m), $d\theta$ is the angle differential unit of the bearing arch along the roadway center, and b is the maintaining bearing arch thickness (m).

$$b = \frac{l \tan \vartheta - D}{\tan \vartheta} \quad (m) \quad (5)$$

According to Equations (1) and (4), N is obtained as follows:

$$N = P \frac{1 + \sin \varphi}{1 - \sin \varphi} b + \frac{1}{2} k^2 b^2 \quad (\text{kN}) \quad (6)$$

where k is the increasing slope of the radial stress, k is 0 in the unstable broken rock mass, l is the bolt effective length (m), and ϑ is the bolt control angle in a fractured rock mass ($^\circ$). Therefore, Equation (6) can be rewritten as follows:

$$N = P \frac{1 + \sin \varphi}{1 - \sin \varphi} \frac{l \tan \vartheta - D}{\tan \vartheta} \quad (\text{kN}) \quad (7)$$

For the ring-shaped bearing arch, using its symmetry, yields the following relations:

$$\sum Y = 0; \int_0^\pi q \sin \theta ds = 2N_0 \quad (8)$$

where q is the bearing capacity of the bearing arch under the first bolt–mesh–shotcrete support, and N_0 is the circumferential direction axial force generated by the bearing arch. From Equations (4) and (8), the following results can be obtained:

$$N_0 = \left(r + \frac{b}{2}\right)q \quad (\text{kN}) \quad (9)$$

when N is equal to N_0 , the bearing arch is in the limit equilibrium state. Combining Equations (5), (7), and (9), we can obtain the following results:

$$q = \frac{2P(1 + \sin \varphi)(l \tan \vartheta - D)}{(2r \tan \vartheta + l \tan \vartheta - D)(1 - \sin \varphi)} \quad (\text{MPa}) \quad (10)$$

By substituting the above equation into Equation (3), the bearing capacity of the bearing arch after the first bolt–mesh–shotcrete support is obtained as follows:

$$q = \frac{2F_b(1 + \sin \varphi)(l \tan \vartheta - D)}{D^2(2r \tan \vartheta + l \tan \vartheta - D)(1 - \sin \varphi)} \quad (\text{MPa}) \quad (11)$$

The support parameters of the bolts used in the second bolt–cable–mesh–shotcrete support are the same as those used in the first bolt–mesh–shotcrete support. Therefore, under the second bolt–cable–mesh–shotcrete support, the bearing capacity, q' , of the bearing arch is as follows:

$$q' = \frac{2F_b(1 + \sin \varphi)(l \tan \vartheta - D)}{D^2(2r \tan \vartheta + l \tan \vartheta - D)(1 - \sin \varphi)} + \frac{2F_c(1 + \sin \varphi)(l' \tan \vartheta - D')}{D'^2(2r \tan \vartheta + l' \tan \vartheta - D')(1 - \sin \varphi)} \quad (\text{MPa}) \quad (12)$$

Subsequently, the bearing capacity of the superimposed coupling strengthening bearing arch formed by a two-layer bolt–shotcrete is as follows:

$$q^{\text{total}} = \frac{4F_b(1 + \sin \varphi)(l \tan \vartheta - D)}{D^2(2r \tan \vartheta + l \tan \vartheta - D)(1 - \sin \varphi)} + \frac{2F_c(1 + \sin \varphi)(l' \tan \vartheta - D')}{D'^2(2r \tan \vartheta + l' \tan \vartheta - D')(1 - \sin \varphi)} \quad (\text{MPa}) \quad (13)$$

where q^{total} is the bearing capacity of superimposed coupling strengthening bearing arch (MPa), F_c is the cable support resistance (kN), D' is the cable spacing (m), and l' is the cable effective length (m).

Combined with the actual production, the basic parameters are determined as follows: $\varphi = 30^\circ$, $\vartheta = 45^\circ$, $l = 2$ m, and $l' = 6$ m. According to Equation (13), the relationship between the bearing capacity of the superimposed coupling strengthening bearing arch and the spacing and support resistance of the bolts (cables) can be obtained, as shown in Figure 8.

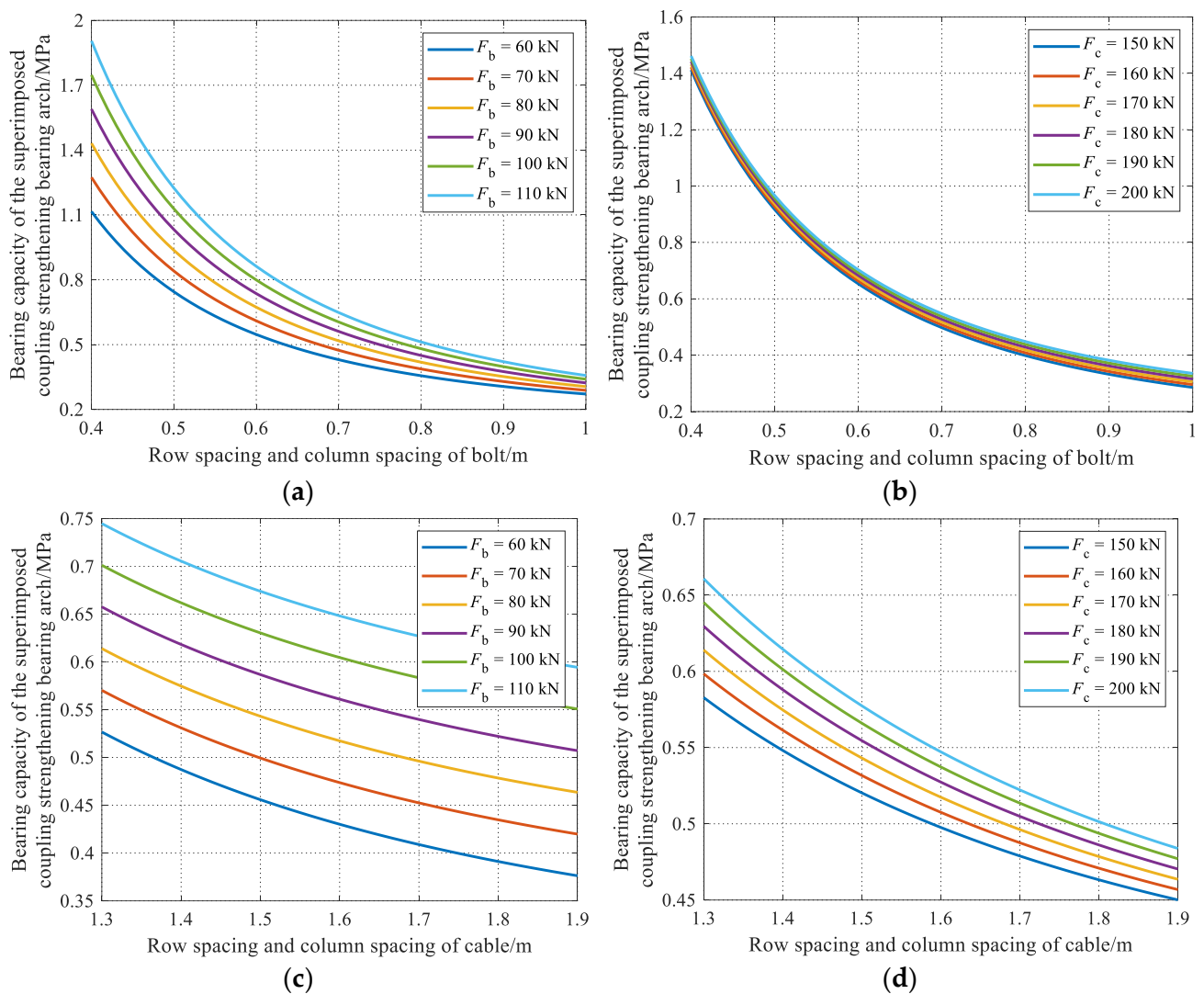


Figure 8. Curves of bearing capacity of superimposed coupling strengthening bearing arch under different influence factors. (a) Curves of bearing capacity and bolt spacing under different bolt support resistances, (b) curves of bearing capacity and bolt spacing under different cable support resistances, (c) curves of bearing capacity and cable spacing under different bolt support resistances, (d) curves of bearing capacity and cable spacing under different cable support resistances.

It can be seen from Figure 8 and Equation (13) that the bearing capacity of the superimposed coupling strengthening bearing arch linearly increased with the increase in the support resistance of the bolts (cables). According to Figure 8a,b, when the bolt spacing was large (0.7–1.0 m), then even if the support resistance of the bolt or cable was high, the superimposed coupling strengthening bearing arch still maintained a low-stress state. With the decrease in the bolt spacing (from 0.7 m to 0.4 m), the bearing capacity of the superimposed coupling strengthening bearing arch increased rapidly in the form of a power function. Taking the bolt support resistance, $F_b = 90$ kN in Figure 8a, as an example, when the bolt spacing decreased from 1 m to 0.7 m, the bearing capacity of the superimposed coupling strengthening bearing arch increased from 0.32 MPa to 0.56 MPa, with an increase of only 75%. When the bolt spacing decreased from 0.7 m to 0.4 m, the bearing capacity of the superimposed coupling strengthening bearing arch increased from 0.56 MPa to 1.59 MPa, with an increase of 183.9%. It can be seen that when the bolt spacing was between 0.7 m and 0.4 m, it was more conducive for high performance of the bearing capacity of the superimposed coupling strengthening bearing arch.

The comparative analysis in Figure 8a,b (or Figure 8c,d) shows that the increase in the bolt support resistance caused the bearing capacity of the superimposed coupling strengthening bearing arch to increase significantly. However, the cable support resistance increase did not significantly change the bearing capacity of the superimposed coupling strengthening bearing arch. Taking the 0.7-m bolt spacing as an example, in Figure 8a, as the bolt support resistance, F_b , increased from 70 kN to 100 kN, the bearing capacity of the superimposed coupling strengthening bearing arch increased from 0.47 MPa to 0.6 MPa, with an increase of 27.7%. However, in Figure 8b, when the cable support resistance, F_c , increased from 160 kN to 190 kN, the bearing capacity curves of the superimposed coupling strengthening bearing arch were nearly coincident, and the bearing capacity was almost unchanged. The comparative analysis in Figure 8a,c (or Figure 8b,d) shows that compared to reducing the cable spacing, reducing the bolt spacing increased the bearing capacity of the superimposed coupling strengthening bearing arch more rapidly. Taking the bolt support resistance, $F_b = 90$ kN, as an example, in Figure 8a, when the bolt spacing decreased from 0.7 m to 0.4 m, the bearing capacity of the superimposed coupling strengthening bearing arch increased from 0.56 MPa to 1.59 MPa, with an increase of 183.9%. Nevertheless, in Figure 8c, when the cable spacing decreased from 1.6 m to 1.3 m, the bearing capacity of the superimposed coupling strengthening bearing arch increased from 0.56 MPa to 0.66 MPa, with an increase of only 17.9%. The above results show that in the superimposed coupling strengthening bearing arch system, compared to the cable bearing arch, changing the support parameters of the bolt bearing arch can significantly change the bearing capacity. Therefore, the setting of the bolt support parameters is particularly important.

Furthermore, in the new combined technology, the shotcrete layer and the bolts work together to produce restraint resistance at the surrounding rock, jointly resisting the roadway's deformation. The thicknesses of the shotcrete layer and the bolt support parameters directly affect the level of restraint resistance. To further optimize the support parameters of the new combined technology, it was essential to determine the thickness of each shotcrete layer. Therefore, mechanical models of the single-layer shotcrete and bolts were established to explore the support principles of the shotcrete layer and bolts for a broken rock mass.

To facilitate the analysis and calculation, the following assumptions were made for this mechanical model: (1) the single-layer shotcrete structure (see Figure 9a) between adjacent bolts on the same level was regarded as the mechanical model of a clamped–clamped beam (see Figure 9b); (2) this clamped–clamped beam is a continuous, homogeneous, isotropic material, which accords with the assumption of elastic mechanics.

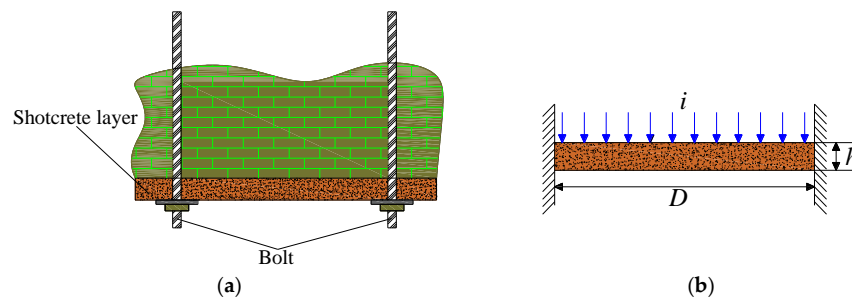


Figure 9. (a) Simplified graph of single-layer shotcrete structure, (b) clamped–clamped beam mechanical model.

According to the Mohr–Coulomb strength criterion,

$$\sigma_1 = \sigma_3 \frac{1 + \sin \varphi}{1 - \sin \varphi} + 2c \frac{\cos \varphi}{1 - \sin \varphi} \quad (\text{MPa}) \quad (14)$$

Because the uniform load i is equal to σ_3 , according to the material mechanics,

$$i = \frac{2h^2\sigma_t}{D^2} \quad (\text{MPa}) \quad (15)$$

where h is the thickness of the single-layer shotcrete (mm), σ_t is the shotcrete strength (MPa), and u is the Poisson ratio.

From Equations (14) and (15), we can obtain the following results:

$$\sigma_1 = \frac{2h^2\sigma_t}{D^2} \cdot \frac{1 + \sin \varphi}{1 - \sin \varphi} + 2c \frac{\cos \varphi}{1 - \sin \varphi} \quad (\text{MPa}) \quad (16)$$

Combined with the production practice, $c = 0.11$ MPa, $\sigma_t = 1.05$ MPa, and $u = 0.3$. By substituting these into Equation (16), the relationship between the bearing capacity of the single-layer shotcrete structure and the bolt spacing and the single-layer shotcrete thickness is obtained, as shown in Figure 10. It can be seen in Figure 10a that when the bolt spacing decreased from 1 m to 0.7 m, even if the thickness of the single-layer shotcrete was large, the bearing capacity of the shotcrete structure increased slowly with the decrease in bolt spacing. When the bolt spacing decreased from 0.7 m to 0.4 m, the bearing capacity of the shotcrete structure increased more obviously with the decrease in the bolt spacing. Taking the single-layer shotcrete thickness, $h = 80$ mm in Figure 10a, as an example, when the bolt spacing decreased from 1 m to 0.7 m, the bearing capacity of the shotcrete structure increased from 0.42 MPa to 0.46 MPa, with an increase of only 9.5%. However, when the bolt spacing decreased from 0.7 m to 0.4 m, the bearing capacity of the shotcrete structure increased from 0.46 MPa to 0.63 MPa, with an increase of 37%. Thus, it is clear that when the bolt spacing was between 0.7 m and 0.4 m, it was more conducive to the high performance of the shotcrete structure's bearing capacity. This result is the same as the reasonable range of the bolt spacing in the superimposed coupling strengthening bearing arch structure, which also shows that the design of the bolt spacing in the primary support scheme is unreasonable. In addition, it can be seen in Figure 10b that the bearing capacity of the single-layer shotcrete structure maintained a low-stress value when the thickness of the single-layer shotcrete was small (from 20 mm to 50 mm). With the increase in the single-layer shotcrete thickness (from 50 mm to 100 mm), the bearing capacity of the shotcrete structure increased rapidly in the form of a power function. However, considering factors such as the rebound rate and economic benefits, the single-layer shotcrete thickness should not be extremely large.

According to the above analysis, the setting of the bolt support parameters is particularly important. A bolt spacing of 0.4–0.7 m and a single-layer shotcrete thickness of 50–100 mm are more conducive to the stability of the surrounding rock than in other cases.

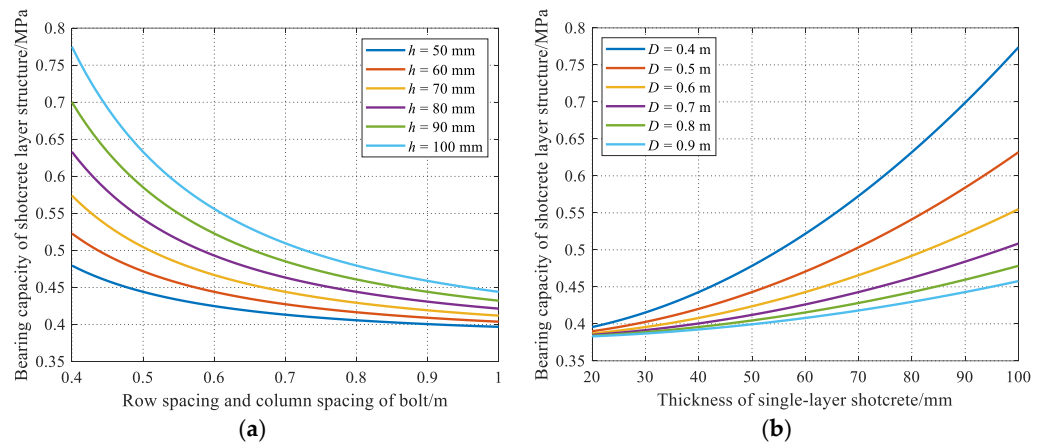


Figure 10. Curves of bearing capacity of shotcrete layer structure under different influence factors. (a) Curves of bearing capacity and bolt spacing under different single-layer shotcrete thicknesses, (b) curves of bearing capacity and single-layer shotcrete thickness under different bolt spacings.

3.2. Technology and Mechanism of Grouting Reinforcement for the Full Cross-Section of Surrounding Rock

The primary support of the roadway intersection is the conventional single-layered bolt–shotcrete support technology. The surrounding rock undergoes fracture repeatedly, and cracks continue to develop in deeper areas impacted by engineering disturbances. Grouting has the effect of plugging the cracks of the surrounding rock and increasing the cohesion between rock blocks, allowing soft and broken surrounding rocks to bond with a certain degree of strength. The ability of the broken surrounding rock to resist dynamic pressure is improved. Grouting makes the surrounding rock of the roadway maintain a high residual grouting pressure. A slurry with a high residual grouting pressure can fill the cracks in a shallow surrounding rock, the gap between a bolt (cable) and a hole in the wall, and deeper fracture areas, forming a network skeleton structure, including a shotcrete layer, dense high-strength bolts (cables), a consolidation slurry, and a rock mass. In addition, the grouting makes the dense high-strength bolts similar to a full-length anchorage, expanding the anchorage scope of the bolts, and further increasing the influence range of the superimposed coupling strengthening bearing arch, as shown in Figure 11a. Grouting also strengthens thick shotcrete structures with a two-layer steel mesh. Among the multiple-layered staggered dense arrangement of bolts, multiple-layered laying of steel meshes, multiple-layered pouring of shotcrete, strengthening support of long cables, and full cross-section grouting, the interaction mechanism of the arching and strengthening support is shown in Figure 11b.

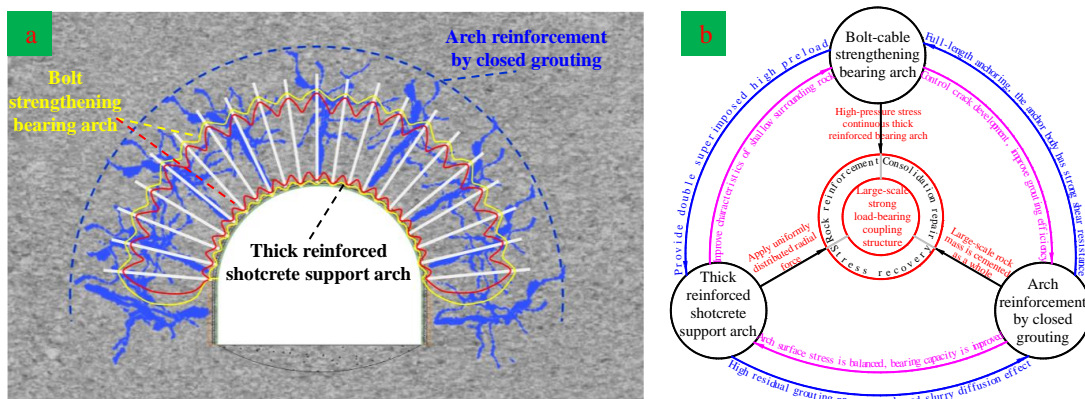


Figure 11. (a) Schematic diagram of surrounding rock grouting reinforcement technology, (b) interaction mechanism of arching and strengthening support.

4. Numerical Analysis for Primary Support and New Support

4.1. Parameters of Primary and New Supports

Under the action of high tectonic stress on the deep coal measure strata, the surrounding rock of the roadway intersection appears soft, broken, and loose and presents rheological features [30,31]. Considering the geological conditions of roadway intersections, combined with theoretical analysis, engineering analogies, and economic benefits, the new support scheme was determined as follows: The first-, second-, and third-layer shotcrete thicknesses were 80 mm, 50 mm, and 50 mm, respectively. The spacing of the bolts in the same layer was 700×700 mm. The bolts in different layers cooperated effectively in space, finally forming the new multiple bolt–shotcrete support technology with a bolt spacing of 350×350 mm and a shotcrete layer 180 mm thick. From the calculation, the bearing capacity of the bearing arch formed by the primary support scheme was 0.17 MPa, whereas that of the superimposed coupling strengthening bearing arch formed by the new support scheme reached 0.57 MPa, an increase of 235%.

In the primary support, the bearing capacity of the bolt bearing arch is low. Combined with the field engineering experience, it was decided to select high-strength bolts with dimensions of $\Phi 22 \times 2400$ mm and spacing of 700×700 mm. When long cables are arranged with small spacing, the compressive stress zone formed by the adjacent cables will overlap in a large area of the surrounding rock, forming a cable bearing arch. In the primary support, the compressive stress zones formed by the adjacent cables cannot be effectively overlapped. They cannot be coupled well with the bolt bearing arch in the shallow surrounding rock. Therefore, based on field engineering experience, it was decided to select cables with dimensions of $\Phi 21.8 \times 8500$ mm and spacing of 1600×1600 mm. Based on the above analysis, in the numerical simulation, the parameters of the bolt (cable) and shotcrete layers in the primary support and new support are listed in Table 1.

Table 1. Parameters of bolt (cable) and shotcrete layer in primary and new supports.

	Bolt	Cable	Shotcrete	Grouting Bolt
Primary scheme	$\Phi 22 \times 2000$ mm Spacing: 800×800 mm	$\Phi 21.8 \times 6500$ mm Spacing: 2000×1800 mm	120 mm	$\Phi 22 \times 2000$ mm Spacing: 1500×1500 mm
New scheme	$\Phi 22 \times 2400$ mm Spacing: 700×700 mm	$\Phi 21.8 \times 8500$ mm Spacing: 1600×1600 mm	180 mm	$\Phi 22 \times 2000$ mm Spacing: 1500×1500 mm

4.2. Numerical Model Generation

Based on the geological conditions of the -760 -m-roadway intersection in the Xingdong coal mine, a numerical model (see Figure 12) was established to investigate the support effect of the surrounding rock in the roadway intersection under the different support conditions. A vertical stress of 19.3 MPa was applied at the top model boundary to simulate the overburden pressure. The bottom boundary of the model was restricted along the vertical direction. The lateral boundary of the model was restricted along the horizontal direction.

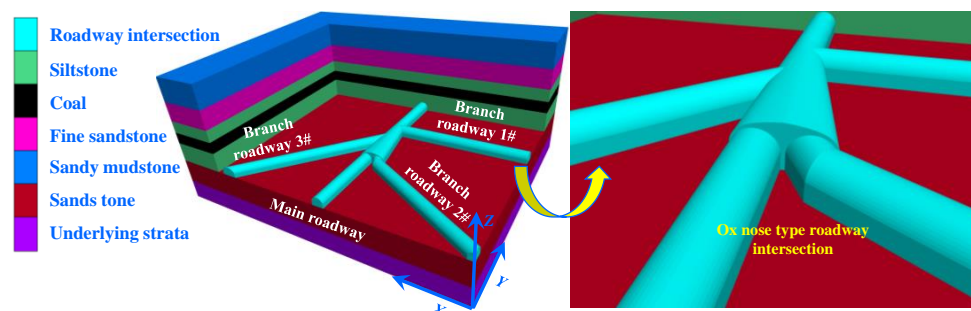


Figure 12. Model of numerical calculation.

The cable and shell structures in the FLAC3D software were used to simulate the bolt (cable) and shotcrete layers, respectively. The Mohr–Coulomb constitutive model was used to simulate the failure of the rock masses. Table 2 lists the main rock parameters.

Table 2. Rock strata properties used in numerical model.

Rock Strata	Density (kg/m ³)	Bulk Modulus (GPa)	Shear Modulus (GPa)	Friction Angle (°)	Cohesion (MPa)	Tensile Strength (MPa)
Sandy mudstone	2400	4.87	2.58	30	1.2	1.10
Fine sandstone	2700	7.87	3.38	30	2.6	2.40
Siltstone	2750	8.82	4.84	31	3.0	2.57
2#Coal	1350	2.35	1.87	20	1.2	0.90
Sandstone	2620	7.50	4.10	32	1.7	1.20

4.3. Numerical Model Results Analysis

4.3.1. Vertical Stress Analysis

The simulated evolutionary processes of the vertical stress around the roadway intersection under the different support conditions are shown in Figure 13.

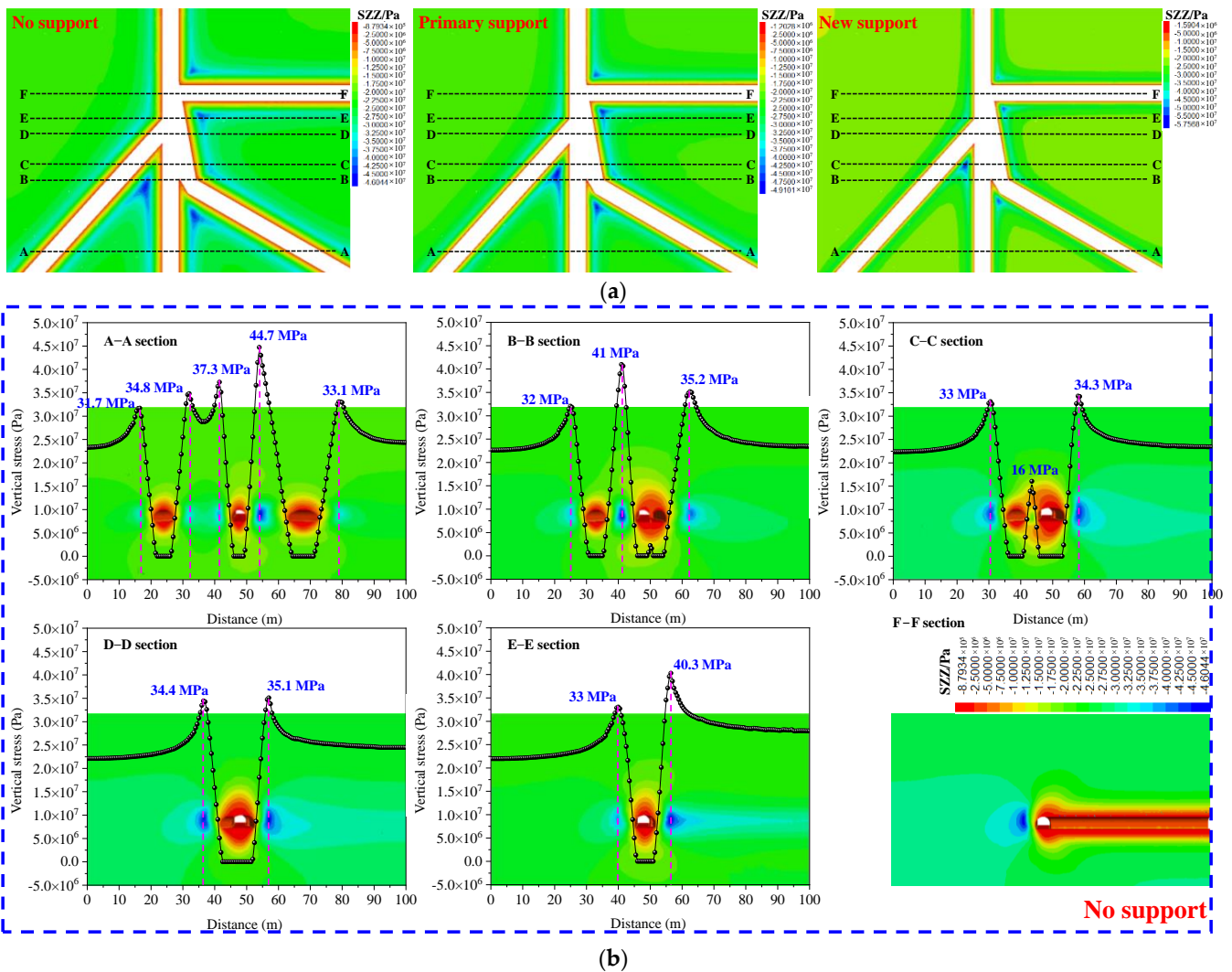


Figure 13. Cont.

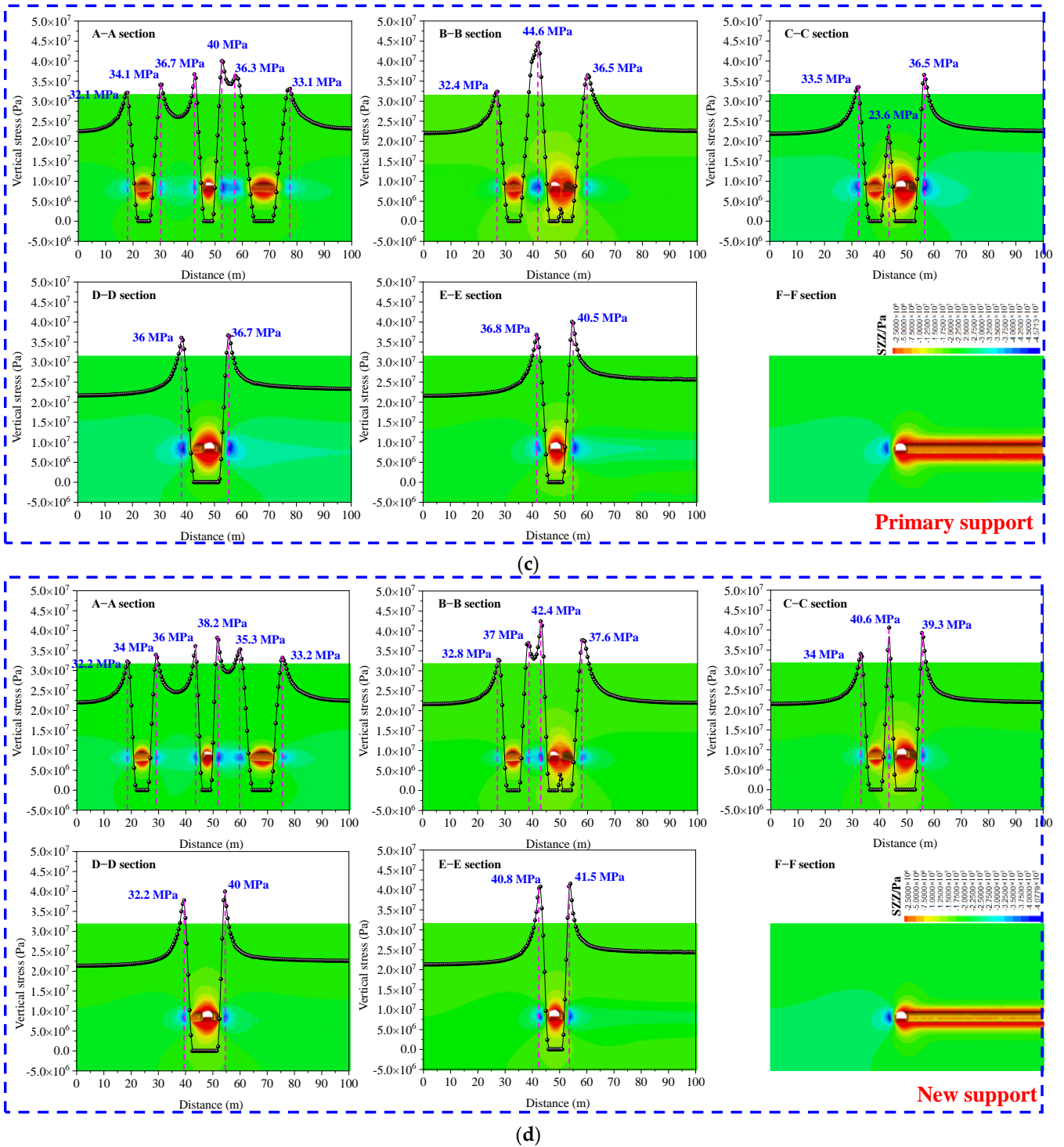
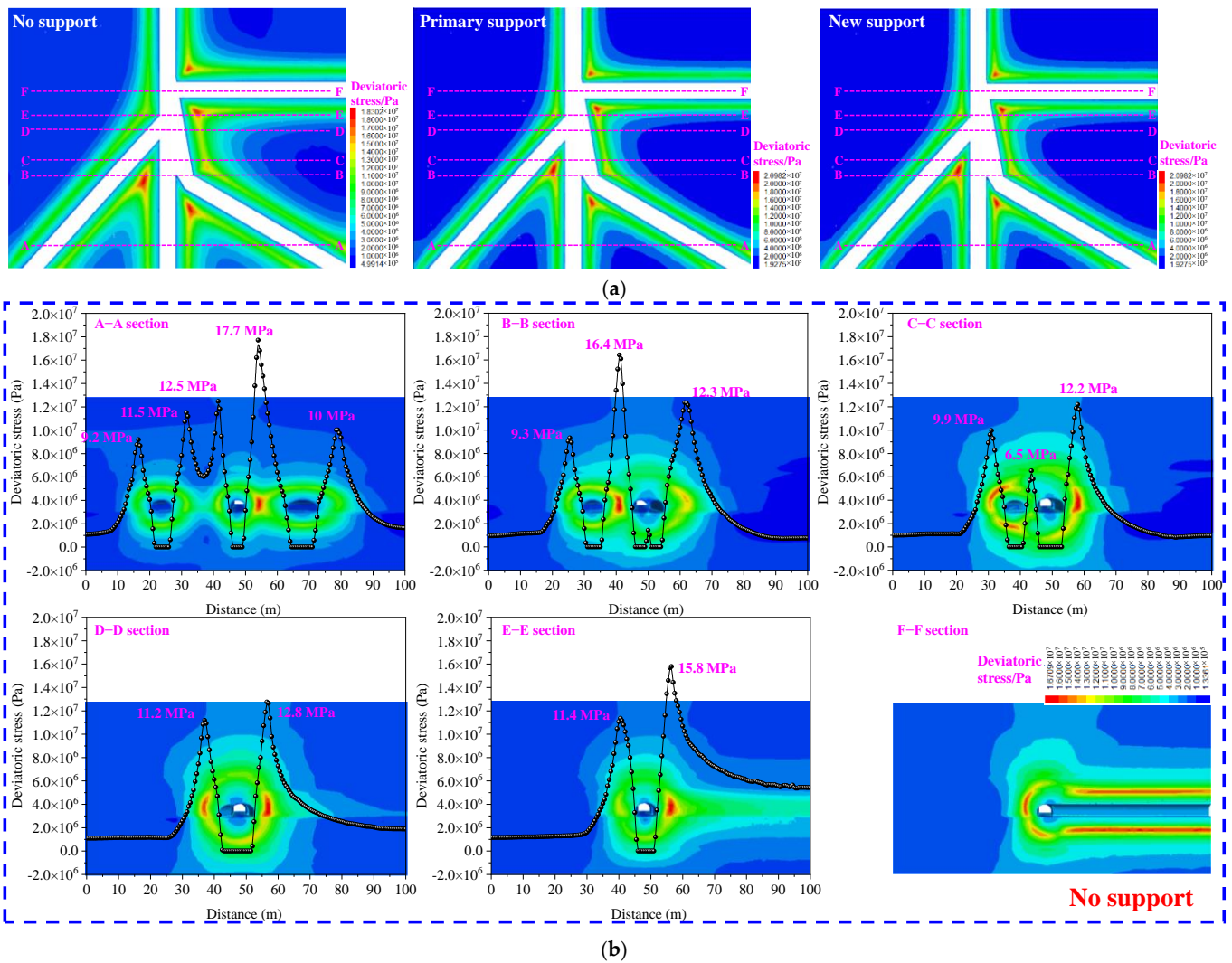


Figure 13. Vertical stress distribution around roadway intersection under the different support conditions. (a) Vertical stress distribution on horizontal plane of roadway under no support, primary support, new support (the letters A to F in each figure indicate roadway sections at different locations). (b) Under the no-support mode, the vertical stress distribution of the roadway’s surrounding rock at different roadway section positions (from A-A section to F-F section). (c) Under the primary support mode, the vertical stress distribution of the roadway’s surrounding rock at different roadway section positions (from A-A section to F-F section). (d) Under the new support mode, the vertical stress distribution of the roadway’s surrounding rock at different roadway section positions (from A-A section to F-F section).

The results show that the roadway intersection is located in a large stress relaxation area under the conditions of excavation without support. After adopting the conventional bolt–shotcrete support scheme, the shallow surrounding rock at the roadway intersection was still in a low-stress area; however, the stress level of the shallow surrounding rock of the roadway was greatly improved after the multi-level bolt–shotcrete support structure was adopted. The application of the new multi-level bolt–shotcrete support structure makes the shallow surrounding rock at the roadway intersection approximately present a triaxial compression state, and the bearing capacity of the shallow surrounding rock was greatly improved, which is conducive to maintaining the long-term stability of the roadway’s surrounding rock.

4.3.2. Deviatoric Stress Analysis

The simulated evolutionary processes of the deviatoric stress around the roadway intersection under the different support conditions are shown in Figure 14.



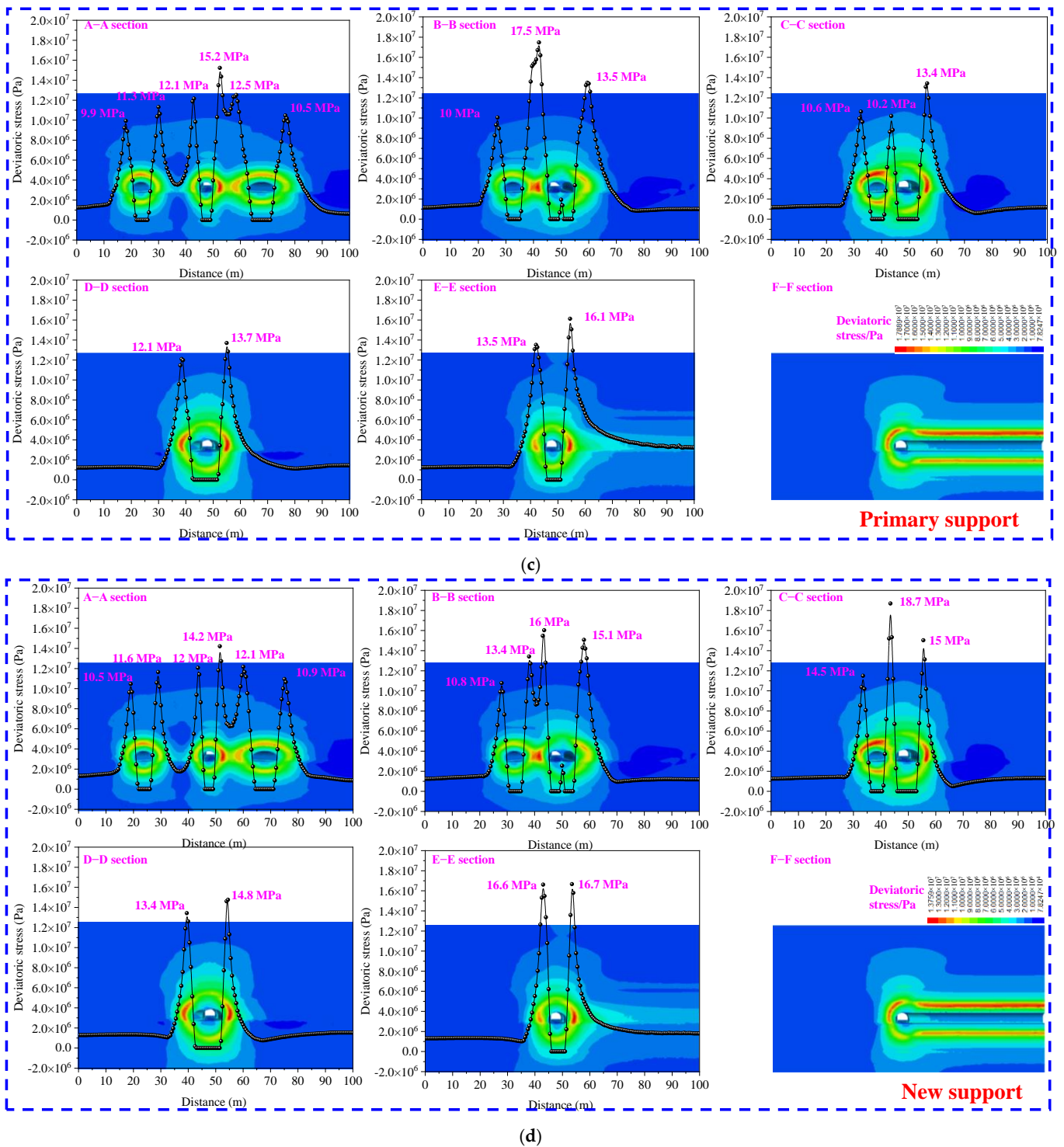


Figure 14. Deviatoric stress distribution around roadway intersection under the different support conditions. (a) Deviatoric stress distribution on horizontal plane of roadway under no support, primary support, and new support (the letters A to F in each figure indicate roadway sections at different locations). (b) Under the no-support mode, the deviatoric stress distribution of the roadway’s surrounding rock at different roadway section positions (from A-A section to F-F section). (c) Under the primary support mode, the deviatoric stress distribution of the roadway’s surrounding rock at different roadway section positions (from A-A section to F-F section). (d) Under the new support mode, the deviatoric stress distribution of the roadway’s surrounding rock at different roadway section positions (from A-A section to F-F section).

The results show that the roadway intersection formed a ring peak zone of deviatoric stress after excavation. With the increase in support strength, the ring peak zone of deviatoric stress gradually moved to the shallow part of the roadway's surrounding rock. More importantly, the transfer distance of the ring peak zone of the deviatoric stress under the traditional bolt–shotcrete support was far less than that of the multi-level bolt–shotcrete support compared to the no-support conditions.

4.3.3. Plastic Zone Analysis

After roadway excavation, the surrounding rock mainly undergoes shear and tensile failure. The maximum plastic zone depth of surrounding rock was used to determine the plastic extent around the excavations (marked as magenta numerals in the following figure). The distribution of the plastic zone depth of each section of the roadway's surrounding rock under different support conditions at the roadway intersection is shown in Figure 15 below:

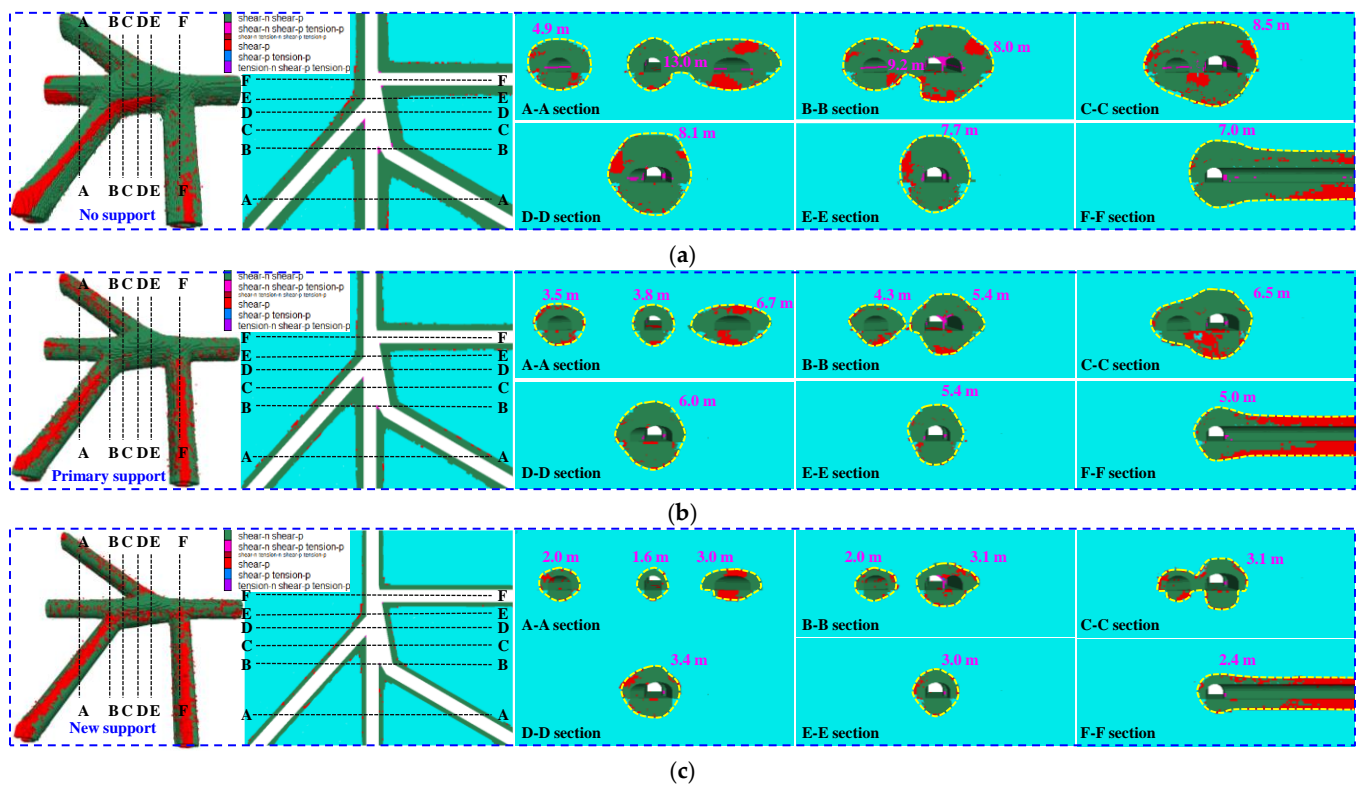


Figure 15. Plastic zone distribution around roadway intersection under different support conditions. (a) Under the no-support mode, the plastic zone distribution of the roadway's surrounding rock at different roadway section positions (from A-A section to F-F section). (b) Under the primary support mode, the plastic zone distribution of the roadway's surrounding rock at different roadway section positions (from A-A section to F-F section). (c) Under the new support mode, the plastic zone distribution of the roadway's surrounding rock at different roadway section positions (from A-A section to F-F section).

The results show that due to the weak lithology, the large buried depth, and the large cross-section of the roadway intersection, the deformation and damage of the roadway intersection are serious under the conditions of excavation without support. After adopting the conventional bolt–shotcrete support scheme, the plastic zone of the surrounding rock of the roadway was only reduced by 23.5~29.8%. However, after the multi-level bolt–shotcrete support structure was adopted, the plastic zone of the surrounding rock of the roadway was reduced by 58~65.7% compared to that without support, and the plastic zone of the surrounding rock of the roadway was reduced by 43.3~52.3% compared to

that of the conventional bolt–shotcrete support, indicating that the support effect was greatly improved.

5. Industrial Test

5.1. Technological Process for New Combined Support Technology

Considering the length of the article, this paper only describes the support scheme of the maximum section A-A profile of the roadway intersection in detail. Detailed steps for the new combined support technology are shown in Figure 16. The detailed technological process is depicted in Figure 17.

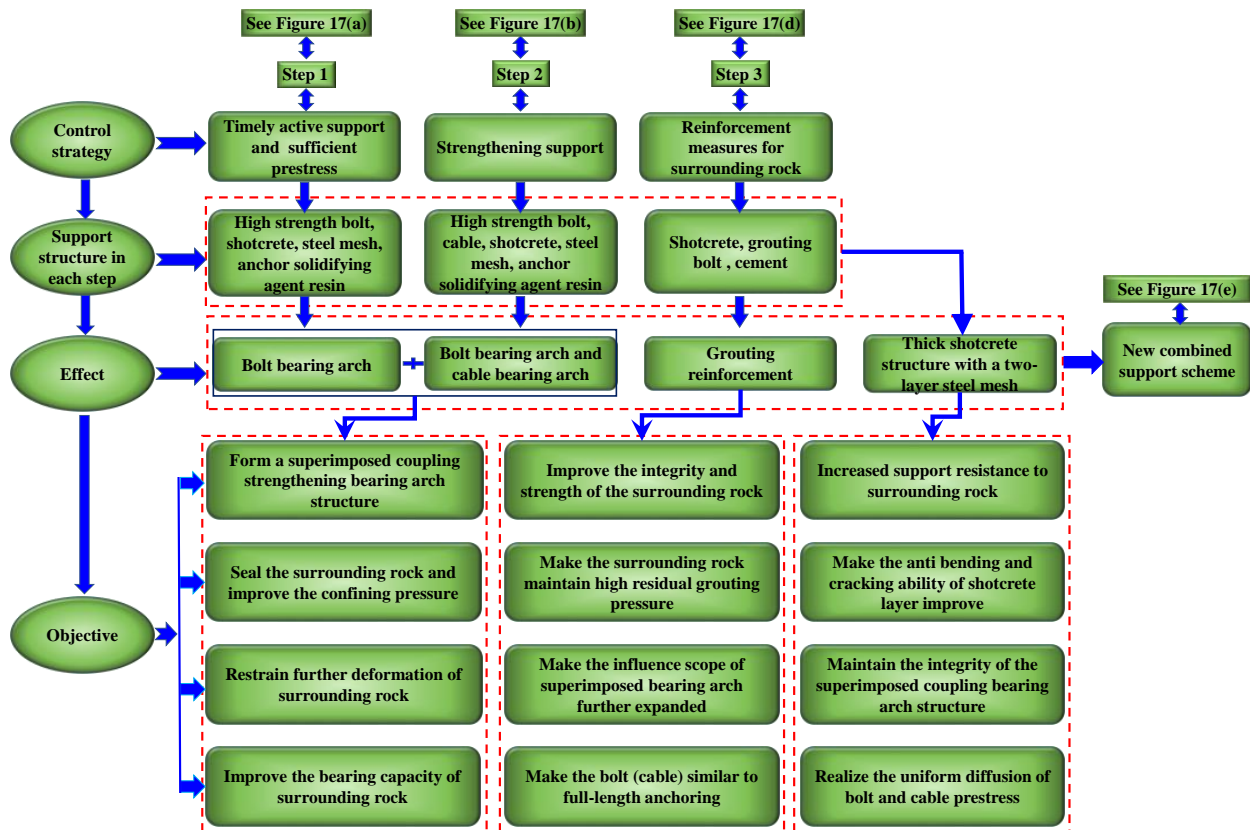


Figure 16. Detailed technological process for new technology.

Step 1: After the roadway is excavated to the specified size, the first layer of shotcrete with a thickness of 80 mm should be sprayed immediately. After the shotcrete layer is solidified, the workers drill holes, lay the first layer of steel mesh, and install the first layer of bolt. This step is the first bolt–mesh–shotcrete support. In this step, $\Phi 22 \times 2400$ mm high-strength bolts are used with a spacing of 700×700 mm. The pre-tightening torque of the bolts is not less than 300 Nm. After the implementation of Step 1, the cross-section support effect of the roadway intersection is as depicted in Figure 17a.

Step 2: A second layer of shotcrete with a thickness of 50 mm is resprayed. A second steel mesh layer is laid, and subsequently, a second layer bolt is installed. Following this, reinforced cables are installed in the roof and sides of the roadway. The second- and the first-layer bolts are staggered in space. This step is the second bolt–cable–mesh–shotcrete support (see Figure 17b). In this step, $\Phi 21.8 \times 8500$ mm high-strength cables are used with a spacing of 1600×1600 mm. The prestress of the cable is 120 kN. The bolt support parameters are the same as those in Step 1. The cross-section effect after the double bolt–shotcrete support at the intersection is shown in Figure 17c.

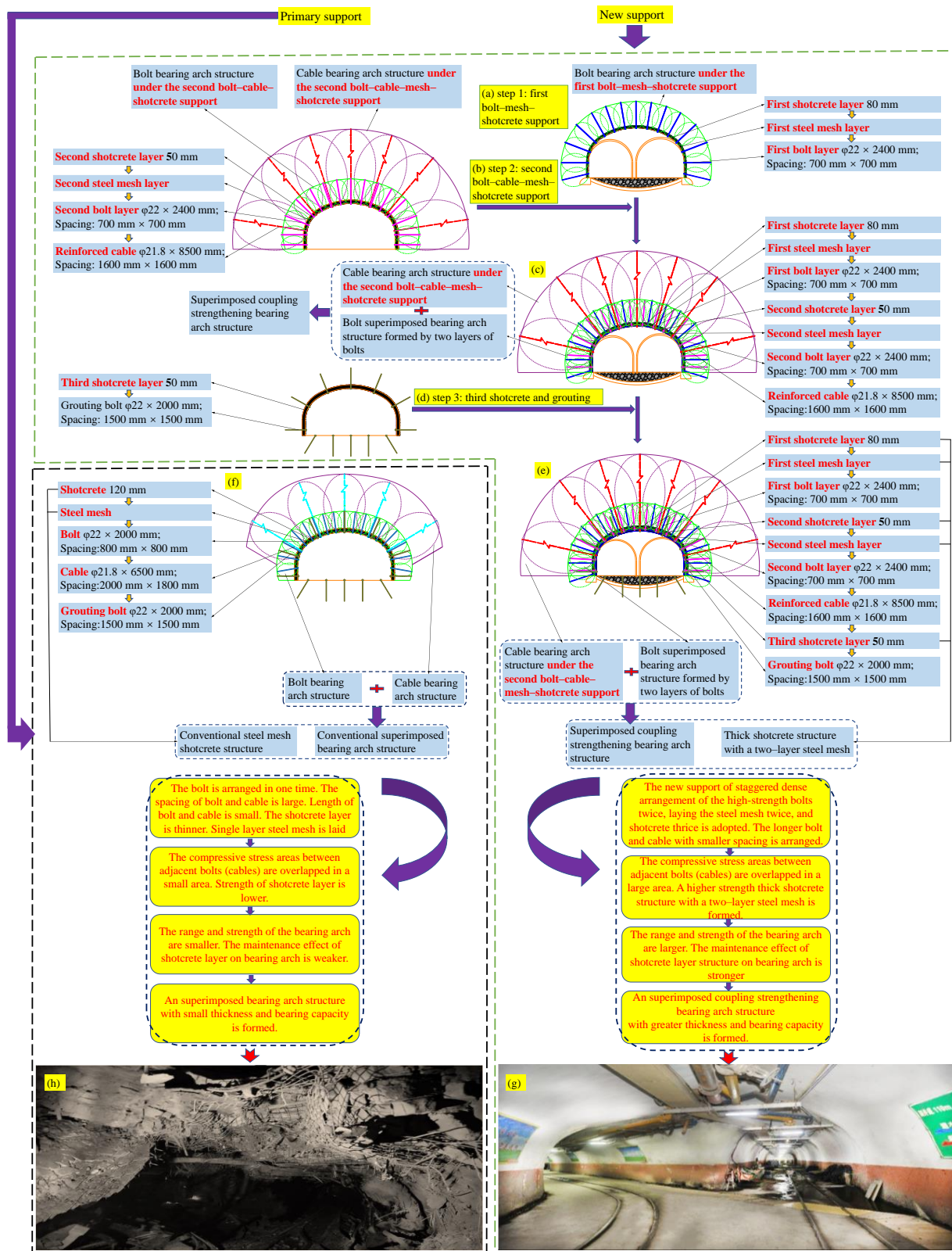


Figure 17. Detailed technological process at roadway intersection. (a) First bolt-mesh-shotcrete support, (b) second bolt-cable-mesh-shotcrete support, (c) superimposed coupling strengthening bearing arch structure, (d) third shotcrete and grouting, (e) final new support effect formed, (f) primary support effect, (g) roadway maintenance effects of the new support schemes, (h) roadway maintenance effects of the primary support schemes.

Step 3: A third layer of shotcrete with a thickness of 50 mm is resprayed. Subsequently, the grouting holes are arranged in the third layer of shotcrete, and the grouting bolt is installed (see Figure 17d). In this step, $\Phi 22 \times 2000$ mm grouting bolts are used with a spacing of $1500 \text{ mm} \times 1500 \text{ mm}$. For the grouting, #425 cement is used, the water–cement ratio is 0.7:1–1:1, and the grouting pressure is 1.5–2.5 MPa.

The support effect of the roadway intersection after grouting is shown in Figure 17e. Compared to the primary support effect (see Figure 17f), the thickness of the arch structure is larger and the bearing capacity is stronger. The roadway maintenance effects of the new and primary support schemes are illustrated in Figure 17g,h, respectively.

After the new combined support technology is implemented, the cross-section of the new support is as shown in Figure 18a, and the corresponding space diagram is depicted in Figure 18b.

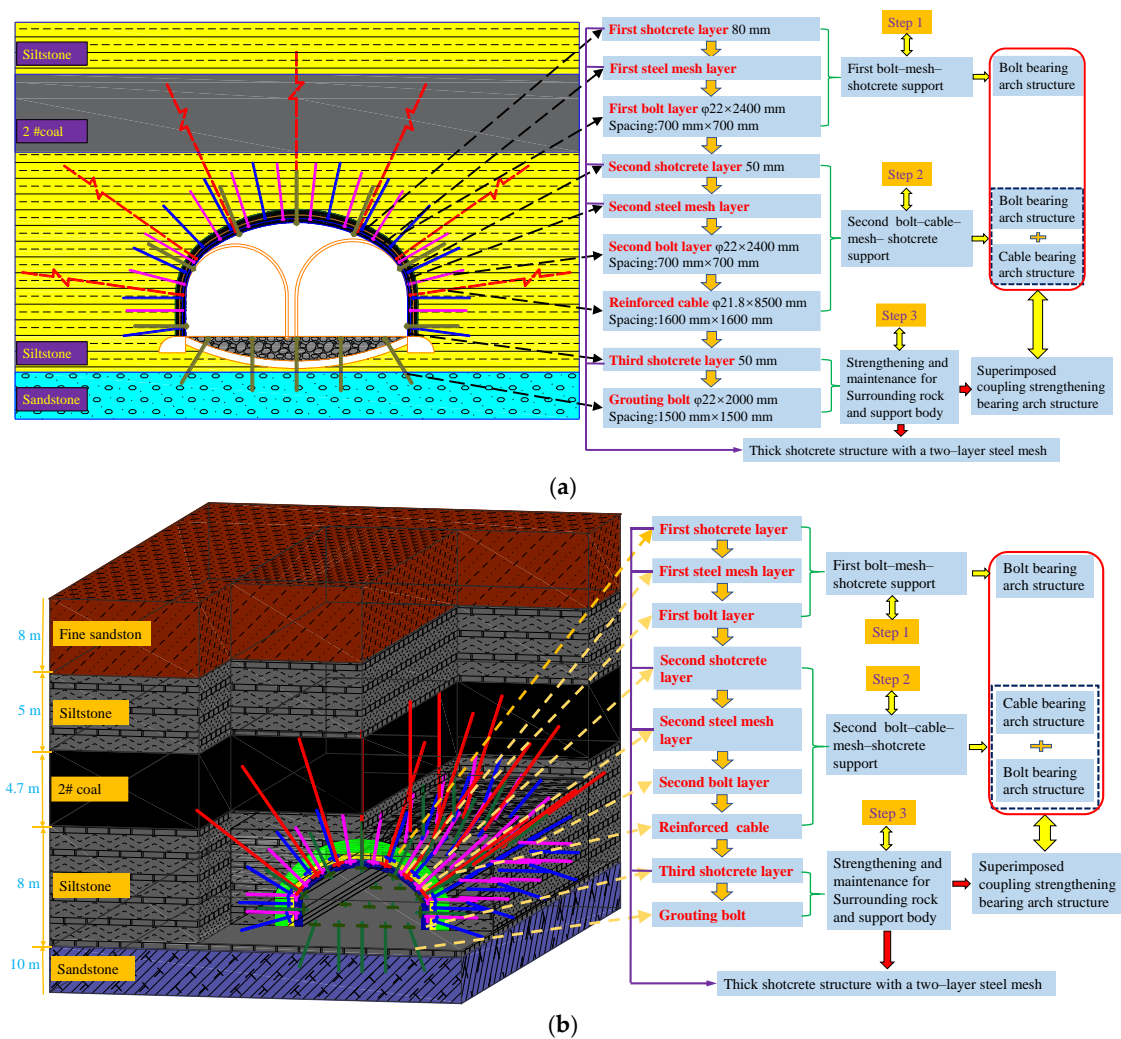


Figure 18. Cross-section diagram and space diagram of new support. (a) Cross-section diagram, (b) space diagram.

5.2. Strata Control Observation at Test Roadway Intersection

(1) Surface convergence

The surrounding rock convergence of the roadway was observed by using telescoping rods and flexible tape. Four pegs were installed in the roadway’s two sides, roof, and floor. The pegs in the roof and the floor were installed in the middle positions to monitor the roof-to-floor convergence. The pegs in the roadway’s two sides were installed 1.6 m away from the roadway floor to monitor the rib-to-rib convergence. The monitoring section was

the A-A profile, as shown in Figure 2c. The monitoring results are presented in Figure 19. The results indicate that the roadway intersection convergences tended to be stable after 26 days. The final roof-to-floor and rib-to-rib convergences of the roadway intersection were 114 mm and 91 mm, respectively. Moreover, the roof-to-floor and rib-to-rib maximum convergence rates of the roadway intersection were 12.3 mm/d and 7.9 mm/d, respectively. The deformations were in the allowable range, which illustrates that the control of the surrounding rock with the new support scheme was effective, as seen in Figure 17g.

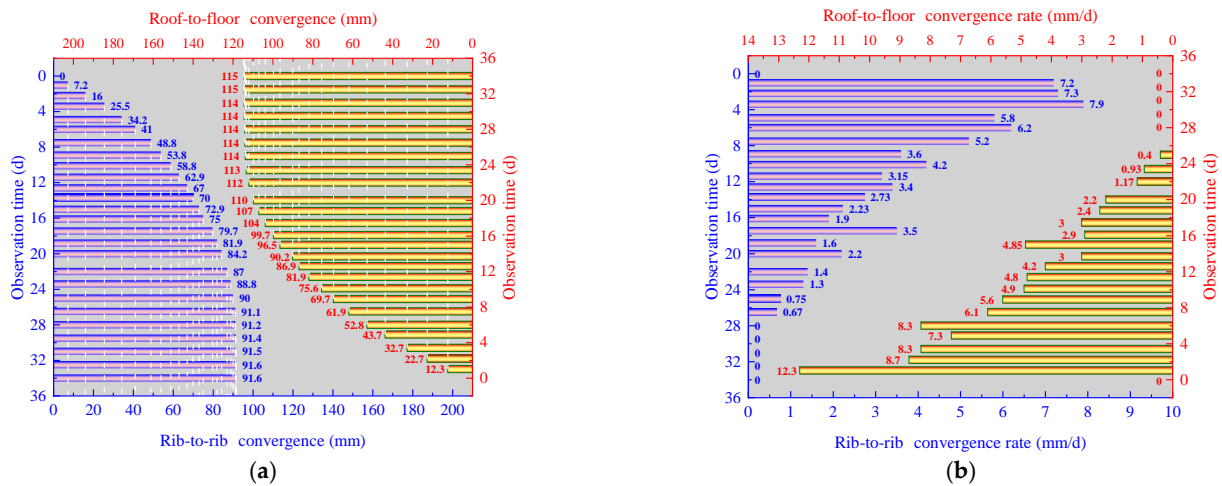


Figure 19. Monitored convergences of roadway intersection. (a) Convergence of roadway roof and side, (b) convergence rate of roadway roof and side.

(2) Borehole drilling results of roadway roof and side

The crack development degree of the roof and side of the roadway was tested by a borehole detector to determine the control effect of the roadway’s surrounding rock under the new support mode. The results are shown in Figure 20.

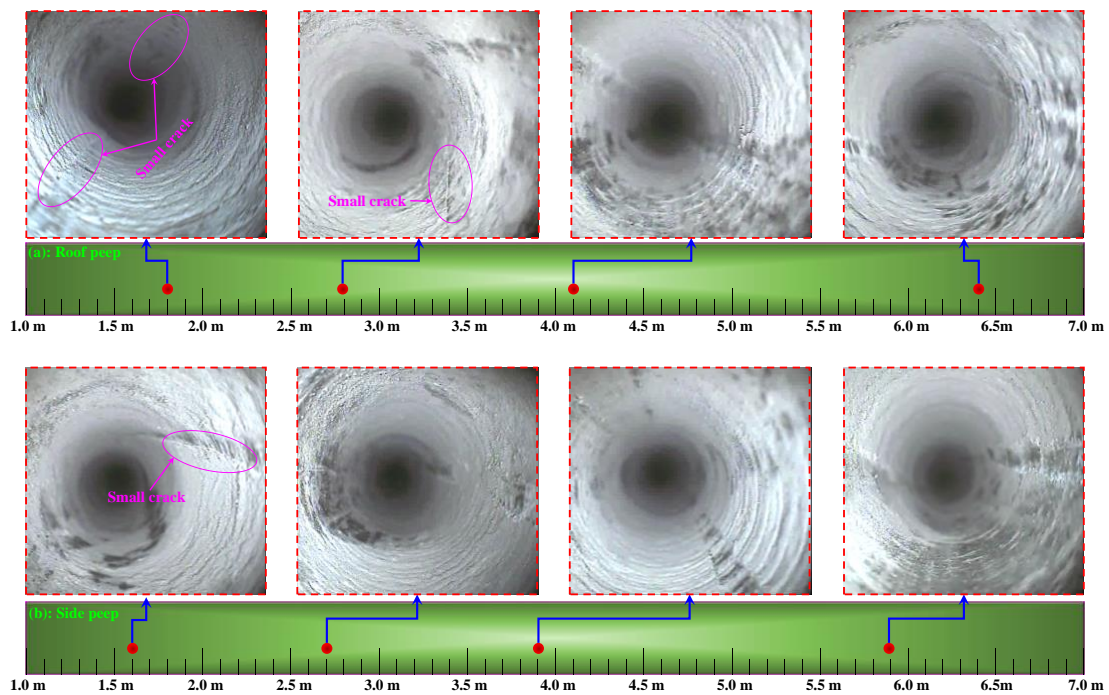


Figure 20. Borehole drilling results of roadway’s roof and side. (a) Roof hole, (b) side hole.

The rock mass above the depth of 3 m in the roadway's roof and side was complete, the lithology was dense, and there was no obvious crack. It can be seen that under the new support mode, the control effect of the roadway's surrounding rock was good, and effective control of the roadway's surrounding rock can be achieved.

6. Conclusions

- (1) The staggered arrangement of the two layers of high-strength bolts forms a thick strengthening bearing arch, improving the stress state of the shallow surrounding rock and weakening the borehole disturbance. The multiple-layered pouring of shotcrete, multiple-layered staggered dense bolts, and interlayer steel meshes form a new type of high-strength bending and crack-resistant reinforced concrete supporting arch structure with built-in multi-layer steel meshes, providing radial overall support stress distribution for the surrounding rock. Grouting is carried out under the conditions of strong sealing of the surrounding rock with a thick reinforced concrete support arch, which further expands the reinforcement scope of the surrounding rock.
- (2) By establishing the mechanical model of the superimposed coupling strengthening bearing arch, the relationship between its bearing capacity and the bolt (cable) spacing and support resistance is obtained. By establishing the shotcrete-layer structure mechanical model, the relationship between its bearing capacity and the bolt (cable) spacing and the single-layer shotcrete thickness is obtained. Analysis of the above two equations shows that when the bolt spacing was between 0.4 m and 0.7 m, it was more conducive to the stability of the surrounding rock. With the increase in the single-layer shotcrete thickness (from 50 mm to 100 mm), the bearing capacity of the shotcrete structure increased rapidly in the form of a power function.
- (3) The numerical simulation results show that, after the multi-level bolt-shotcrete support structure was adopted, the overall stress level of the shallow surrounding rock at the roadway intersection was improved, the bearing capacity of the shallow rock mass was improved, the ring peak zone of the deviatoric stress of the surrounding rock at the roadway intersection was largely transferred to the shallow part, and the plastic zone of the surrounding rock of the roadway was reduced by 43.3~52.3% compared to that of the conventional bolt-shotcrete support.
- (4) After the new combined support technology process was adopted, the roadway intersection convergences tended to be stable after 26 days, the final roof-to-floor and rib-to-rib convergences of the roadway intersections were 114 mm and 91 mm, respectively. Moreover, the maximum roof-to-floor and rib-to-rib convergence rates of the roadway intersection were 12.3 mm/d and 7.9 mm/d, respectively. These results prove that the new combined support technology could achieve long-term stability of the surrounding rock of the deep roadway, avoid frequent expansions and renovations of the roadway, and also save a lot of maintenance costs, ensuring the normal production of the working face.

7. Discussion

Conventional bolt-shotcrete support technology is usually single-layered, which does not meet the requirements of strength and stiffness for roadway support. Therefore, the new combined support technology, including a multiple-layered staggered dense arrangement of bolts, multiple-layered laying of steel meshes, multiple-layered pouring of shotcrete, strengthening support of long cables, and full cross-section grouting, is proposed. Compared to the previous single-layered bolt-shotcrete support, this new technology has the following characteristics and advantages: (1) The staggered arrangement of the two layers of high-strength bolts forms a thick strengthening bearing arch, which greatly improves the stress state of the shallow surrounding rock. (2) The multiple-layered pouring of shotcrete, multiple-layered staggered dense bolts, and interlayer steel meshes form a new type of high-strength bending and crack-resistant reinforced concrete supporting arch structure with built-in multi-layer steel meshes, providing radial overall support stress

distribution for the surrounding rock. (3) Grouting is carried out under the conditions of strong sealing of the surrounding rock with a thick reinforced concrete support arch, which further expands the reinforcement scope of the surrounding rock. In this study, we established a mechanical model of the superimposed coupling strengthening bearing arch and the shotcrete layer structure, analyzed the support mechanism of this new technology, and conducted research on the vertical stress, deviator stress, and plastic zone depth distribution of the roadway's surrounding rock under different support conditions. Finally, this technology was successfully applied in the field. In future research work, we will focus on the research and development of the performance improvement of support materials related to this technology, such as the bolts, cables, mesh, and shotcrete.

Author Contributions: Writing—original draft preparation, Z.J.; writing—review and editing, D.C.; supervision, S.X.; funding acquisition, S.X. and D.C. All authors have read and agreed to the published version of the manuscript.

Funding: This research was funded by the National Natural Science Foundation of China (Nos. 52074296 and 52004286), the China Postdoctoral Science Foundation (No. 2020T130701), and the Fundamental Research Funds for the Central Universities (Nos. 2022XJNY02 and 2022YJSNY18).

Institutional Review Board Statement: Not applicable.

Informed Consent Statement: Not applicable.

Data Availability Statement: The datasets generated or analyzed during the current study are available from the corresponding author upon reasonable request.

Acknowledgments: The author team thanks the field technicians for providing the field test conditions and the ground pressure observation conditions.

Conflicts of Interest: The authors declare that they have no conflict of interest.

References

1. Wang, Q.W.; Feng, H.; Tang, P.; Peng, Y.T.; Li, C.A.; Jiang, L.S.; Mitri, H.S. Influence of yield pillar width on coal mine roadway stability in western china: A case study. *Processes* **2022**, *10*, 251. [[CrossRef](#)]
2. Ma, C.Q.; Wang, P.; Jiang, L.S.; Wang, C.S. Deformation and control countermeasure of surrounding rocks for water-dripping roadway below a contiguous seam goaf. *Processes* **2018**, *6*, 77. [[CrossRef](#)]
3. Chang, J.C.; He, K.; Pang, D.D.; Li, D.; Li, C.M.; Su, B.J. Influence of anchorage length and pretension on the working resistance of bolt based on its tensile characteristics. *Int. J. Coal Sci. Technol.* **2021**, *8*, 1384–1399. [[CrossRef](#)]
4. Chen, J.H.; Zhao, H.B.; He, F.L.; Zhang, J.W.; Tao, K.M. Studying the performance of fully encapsulated bolts with modified structural elements. *Int. J. Coal Sci. Technol.* **2021**, *8*, 64–76. [[CrossRef](#)]
5. Liu, P.Z.; Gao, L.; Zhang, P.D.; Wu, G.Y.; Wang, C.; Ma, Z.Q.; Kong, D.Z.; Kang, X.T.; Han, S. A case study on surrounding rock deformation control technology of gob-side coal-rock roadway in inclined coal seam of a mine in Guizhou, China. *Processes* **2022**, *10*, 863. [[CrossRef](#)]
6. Xie, S.R.; Jiang, Z.S.; Chen, D.D.; Wang, E.; Lv, F. A new pressure relief technology by internal hole-making to protect roadway in two sides of deep coal roadway: A case study. *Rock Mech. Rock Eng.* **2023**, *56*, 1537–1561. [[CrossRef](#)]
7. Chen, D.D.; Guo, F.F.; Li, Z.J.; Ma, X.; Xie, S.R.; Wu, Y.Y.; Wang, Z.Q. Study on the influence and control of stress direction deflection and partial-stress boosting of main roadways surrounding rock and under the influence of multi-seam mining. *Energies* **2022**, *15*, 8257. [[CrossRef](#)]
8. Fu, Q.; Yang, K.; He, X.; Liu, Q.J.; Wei, Z.; Wang, Y. Destabilization mechanism and stability control of the surrounding rock in stope mining roadways below remaining coal pillars: A case study in buertai coal mine. *Processes* **2022**, *10*, 2192. [[CrossRef](#)]
9. Li, G.C.; Sun, Y.T.; Zhang, J.F.; Zhang, Q.J.; Sun, C.L.; Zhang, S.H.; Bi, R.Y. Experiment and application of coalcrete on roadway stability: A comparative analysis. *Adv. Mater. Sci. Eng.* **2020**, *2020*, 6813095. [[CrossRef](#)]
10. Ma, Q.; Zhang, Y.D.; Zhang, X.R.; Li, Z.X.; Song, G.Y.; Cheng, J.Y.; Gao, K.D. The failure law and control technology of large-section roadways in gently inclined soft coal seams. *Processes* **2022**, *10*, 1993. [[CrossRef](#)]
11. Xie, S.R.; Wang, E.; Chen, D.D.; Jiang, Z.S.; Li, H.; Liu, R.P. Collaborative control technology of external anchor-internal unloading of surrounding rock in deep large-section coal roadway under strong mining influence. *J. China Coal Soc.* **2022**, *47*, 1946–1957.
12. Xie, S.R.; Wu, Y.Y.; Chen, D.D.; Liu, R.P.; Han, X.T.; Ye, Q.C. Failure analysis and control technology of intersections of large-scale variable cross-section roadways in deep soft rock. *Int. J. Coal Sci. Technol.* **2022**, *9*, 19. [[CrossRef](#)]
13. Chen, D.D.; Wu, Y.Y.; Xie, S.R.; GUo, F.F.; He, F.L.; Liu, R.P. Reasonable location of stopping line in close-distance underlying coal seam and partition support of large cross-section roadway. *Int. J. Coal Sci. Technol.* **2022**, *9*, 55. [[CrossRef](#)]

14. Yu, W.J.; Li, K. Deformation mechanism and control technology of surrounding rock in the deep-buried large-span chamber. *Geofluids* **2020**, *2020*, 8881319. [[CrossRef](#)]
15. Xie, S.R.; Jiang, Z.S.; Chen, D.D.; Wang, E. Study on zonal cooperative control technology of surrounding rock of super large section soft rock chamber group connected by deep vertical shaft. *Adv. Civ. Eng.* **2022**, *2022*, 4220998. [[CrossRef](#)]
16. Shi, S.; Miao, Y.C.; Wu, H.K.; Xu, Z.P.; Liu, C.W. The stress evolution of adjacent working faces passing through an abandoned roadway and the damage depth of the floor. *Energies* **2022**, *15*, 5824. [[CrossRef](#)]
17. Qin, B.B.; He, F.L.; Zhang, X.B.; Xu, X.H.; Wang, W.; Li, L.; Dou, C. Stability and control of retracement channels in thin seam working faces with soft roof. *Shock Vib.* **2021**, *2021*, 8667471. [[CrossRef](#)]
18. Xia, Z.; Yao, Q.L.; Meng, G.S.; Xu, Q.; Tang, C.J.; Zhu, L.; Wang, W.N.; Shen, Q. Numerical study of stability of mining roadways with 6.0-m section coal pillars under influence of repeated mining. *Int. J. Rock Mech. Min. Sci.* **2021**, *138*, 104641. [[CrossRef](#)]
19. Yu, Y.; Wang, X.Y.; Bai, J.B.; Zhang, L.Y.; Xia, H.C. Deformation mechanism and stability control of roadway surrounding rock with compound roof: Research and application. *Energies* **2020**, *13*, 1350. [[CrossRef](#)]
20. Hu, C.J.; Han, C.L.; Wang, L.X.; Zhao, B.F.; Yang, H.Q. Cooperative control mechanism of efficient driving and support in deep-buried thick top-coal roadway: A case study. *Energies* **2022**, *15*, 4349. [[CrossRef](#)]
21. Hammer, A.L.; Thewesa, M.; Galler, R. Time-dependent material behaviour of shotcrete—New empirical model for the strength development and basic experimental investigations. *Tunn. Undergr. Space Technol.* **2020**, *99*, 103238. [[CrossRef](#)]
22. Zhu, C.L.; Zhou, N.; Guo, Y.B.; Li, M.; Cheng, Q.Q. Effect of doped glass fibers on tensile and shear strengths and microstructure of the modified shotcrete material: An experimental study and a simplified 2d model. *Minerals* **2021**, *11*, 1053. [[CrossRef](#)]
23. Zhang, H.B. Preparation and Performance of Fast-Setting and Rapid-High-Strength Concrete. Ph.D Thesis, Chongqing University, Chongqing, China, 2014.
24. Malmgren, L.; Nordlund, E. Interaction of shotcrete with rock and bolts—A numerical study. *Int. J. Rock Mech. Min. Sci.* **2008**, *45*, 538–553. [[CrossRef](#)]
25. Sjolander, A.; Hellgren, R.; Malm, R.; Ansell, A. Verification of failure mechanisms and design philosophy for a bolt-anchored and fibre-reinforced shotcrete lining. *Eng. Fail. Anal.* **2020**, *116*, 104741. [[CrossRef](#)]
26. Naithani, A.K.; Jain, P.; Rawat, D.S.; Singh, L.G. Rock mass characterization for the underground surge pool cavern—A case study, India. *J. Geol. Soc. India* **2020**, *96*, 265–271. [[CrossRef](#)]
27. Basarir, H.K.; Sun, Y.T.; Li, G.C. Gateway stability analysis by global-local modeling approach. *Int. J. Rock Mech. Min. Sci.* **2019**, *113*, 31–40. [[CrossRef](#)]
28. Panda, M.K.; Mohanty, S.; Pingua, B.M.P.; Mishra, A.K. Engineering geological and geotechnical investigations along the head race tunnel in Teesta Stage-III hydroelectric project, India. *Eng. Geol.* **2014**, *181*, 297–308. [[CrossRef](#)]
29. Yu, W.J.; Gao, Q.; Zhu, C.Y. Study of strength theory and application of overlap arch bearing body for deep soft surrounding rock. *Chin. J. Rock Mech. Eng.* **2010**, *29*, 2134–2142.
30. Wang, Q.; He, M.C.; Li, S.C.; Jiang, Z.H.; Wang, Y.; Qin, Q.; Jiang, B. Comparative study of model tests on automatically formed roadway and gob-side entry driving in deep coal mines. *Int. J. Min. Sci. Technol.* **2021**, *31*, 591–601. [[CrossRef](#)]
31. Sun, Y.T.; Li, G.C.; Zhang, J.F.; Qian, D.Y. Stability control for the rheological roadway by a novel high-efficiency jet grouting technique in deep underground coal mines. *Sustainability* **2019**, *11*, 6494. [[CrossRef](#)]

Disclaimer/Publisher's Note: The statements, opinions and data contained in all publications are solely those of the individual author(s) and contributor(s) and not of MDPI and/or the editor(s). MDPI and/or the editor(s) disclaim responsibility for any injury to people or property resulting from any ideas, methods, instructions or products referred to in the content.